Dissertation for the degree of Philosophiae Doctor

Li Zheng

Preparation for Liquid-Liquid Extraction Studies of Dubnium Using Homologue Models with the SISAK System

Department of Chemistry
Faculty of Mathematics and Natural Sciences
University of Oslo
2007

Series of dissertations submitted to the
Faculty of Mathematics and Natural Sciences, University of Oslo.
No. 657

ISSN 1501-7710

Cover: Inger Sandved Anfinsen.
Printed in Norway: AiT e-dit AS, Oslo, 2007.

Produced in co-operation with Unipub AS.
The thesis is produced by Unipub AS merely in connection with the
thesis defence. Kindly direct all inquiries regarding the thesis to the copyright
holder or the unit which grants the doctorate.

Unipub AS is owned by
The University Foundation for Student Life (SiO)

Preface

Nearly four years have passed since the start of this work. The initiation of this thesis was a big challenge to me. During the touching and unforgettable days and years, a large number of people have been involved, and I am most grateful to them for all the help and support they have given me.

First of all, I wish to express my great gratitude to my supervisor Professor Jon Petter Omtvedt for giving me such an opportunity to pursue a Ph.D degree. It was you who had patiently guided me through the most difficult starting stage of the “long march” and had consistently offered me your considerate and generous help and support in every respect whenever I needed. Also my supervisor Professor and Doctor Tur Bjørnstad should be gratefully acknowledged for having always given timely reply and prompt attention to all the questions which I had taken interest in.

I am greatly indebted to Professor emeritus Jorolf Alstad for his sincere and generous help and consistent attention and encouragement in both my life and study over the years. You have been taken as my best friend and mentor.

A special thank goes to Dr Håvar Gausemel. You have always showed me your patient and excellent tutorship for every question that I had asked. Your wonderful instruction for my skiing practice and your generous contribution to the delicious cakes have always been in my mind.

My gratitude goes to everyone of Oslo SISAK group for their excellent help during my study, especially Fredrik for his constructive suggestion and considerate assistant to the experiments.

My gratitude also goes to Jacklyn Gate for discussions on the work and help in various computer programs.

Operator Eivind Olsen at the Oslo Cyclotron Laboratory and staff are acknowledged for providing high quality and steady beams during the experiments

Financial support from Norwegian Research Council (Project No. 166744/V30) and from the Quota Programme is also greatly appreciated. Moreover, I am heartily grateful to Ms. Michele Nysæter, the International Student Adviser, for having always offered me her helpful advice on financial problems.

I wish to thank many of my other friends for contribution in each of their own ways, though not directly related to my work, but no one will be forgotten, though no one is mentioned here.

Finally, I wish to thank my beloved husband and son for their patience, understanding and support over the years. I want to say to them here: you deserve my deepest love and respect.

Contents

Abstract……iii

List of Papers……v

1 Introduction 1

1.1 Transactinides 1

1.2 SISAK 6

1.3 Objectives 7

2 Background 9

2.1 Chemical Investigation of Dubnium 10

2.2 Chemical Investigation of Superheavy Elements with SISAK 12

3 Methods and Instrumentation 15

3.1 Production of Transactinides 15

Target Chamber 16

3.2 Preseparation and Transportation of Nuclear Reaction Products 18

3.2.1 Physical Preseparator BGS and the Recoil Transfer Chamber (RTC) 18

3.2.2 Gas-jet 20

3.3 Instrumentation of Transactinide Chemistry 22

3.3.1 Gas-phase System 22

3.3.2 Aqueous-phase Systems 24

3.3.3 SISAK System 26

4 Experimental Procedures 37

4.1 Procedure in Model Experiments 37

4.1.1 Batch Experiments and Measurement 37

4.1.2 SISAK on-line Experiments 39

4.2 Procedure in TAE Experiments 41

5 Results and Discussion 45

5.1 Studies on Extraction of Nb, Ta and Pa from H_2SO_4 45
5.1.1 Distribution Ratio of Nb, Ta and Pa in H_2SO_4/TOA system 46
5.1.2 Effect of TOA on the Distribution Ratio of Nb, Ta and Pa 47
5.1.3 Extraction Kinetics of Pa, Nb and Ta in the H_2SO_4 /TOA System 54
5.1.4 The Cluster Dissolution Efficiency 57
5.1.5 Dependence of the Concentration of H^+, HSO_4^- and SO_4^{2-} on H_2SO_4 Concentration 58
5.1.6 The Extraction of Ta and Nb in the H_2SO_4/TOA System with HF Present 59
5.1.7 The Extraction of Ta and Nb into Aliquat 336 in Toluene from H_2SO_4 with or without H_2O_2 Present 61
5.2 Influence of KCl from Gas-jet on the Extraction 67
5.3 SISAK Rutherfordium Experiments 68
6 Conclusions 71
References
Appendix
A1. Calculation of Distribution Ratio (D or D-values)
a. Batch Experiments
b. SISAK on-line Experiments
A2. Phase Separation and Phase Purity
A3. Extraction Mechanism
A4. Hydrolysis
A5. The Calculation of the Amount of H^+, HSO_4^- and SO_4^{2-} in various H_2SO_4 Solutions
A6. 88″ Cyclotron Beam Time Request Form, Detector Tests as a Precursor to Dubnium Chemistry with the SISAK Liquid-Liquid Extraction System

Abstract

Tracers of Nb, Ta, and the pseudo-homologue Pa were used to model the chemical behaviour of dubnium in the development of suitable liquid-liquid extraction systems for the SISAK centrifuge system. Extraction from sulphuric acid solutions into trioctyl amine in toluene and into Aliquat 336 in toluene were investigated as chemical separation systems. Distribution ratios for the homologues and the protactinium tracer, ^{233}Pa, were measured in batch experiments, whereas short-lived cyclotron-produced tracers of Nb and Ta were measured in on-line separations using the SISAK system. SISAK is an automated centrifuge system purpose built to perform fast liquid-liquid extractions of short-lived nuclei. The results establish the optimal conditions for a SISAK dubnium experiment to explore its chemical properties in solutions relating to those of niobium and tantalum.

Addition of H_2O_2 to the Aliquat 336/H_2SO_4 system was investigated as part of this work. The addition suppresses the extraction of Nb. And also Ta, but to a lesser extent. This selective hydrogen peroxide complex formation might serve as the basis for an alternative way to investigate the complexing behaviour of Db.

Part of the work presented here is from participation in a SISAK experiment on ^{257}Rf. In this experiment the distribution ratio for extraction into trioctyl amine in toluene from sulphuric acid was determined. The practical experience gained from the Rf experiment was important to ensure that the liquid-liquid extraction system developed here for dubnium is realistic, and furthermore was invaluable in understanding all the necessary requirements and conditions for performing such a complex experiment. The Rf experiments used for the first time a two-step extraction procedure with direct detection of alpha activity in both organic phases. Consequently, the distribution ratio can be determined without knowledge of the amount of activity entering the SISAK system, thereby reducing the uncertainty in the distribution measurement significantly.

Due to the high amounts of liquid consumed by the SISAK system during transactinide experiments, which typically lasts several days, recycling of chemicals is necessary. This results in build-up of KCl in the aqueous phase (from the KCl-aerosol particles used as carriers in the gas jet). Thus, in a separate study the influence of KCl on the distribution ratios for zirconium and hafnium was determined to be negligible for the 5-time recycling currently used for the aqueous phase. It can, however, become a problem if the aqueous phase is more extensively recycled.

List of Papers

Paper I.

Zheng, L., Alstad, J., Bjørnstad, T., Polakova, D., Stavsetra, L., Omtvedt, J. P., E*xtraction of Nb and Ta, Homologues of Db, from Sulphuric Acid Solutions with TOA in Toluene Using SISAK*, having been accepted by *Radiochimica. Acta*.

Paper II.

Zheng, L., Alstad, J., Bjørnstad, T., Opel, K., Sabelnikov, A. V., Omtvedt, J. P., *SISAK Extraction of Nb and Ta, the Homologues of Db, into Aliquat 336 in Toluene from Sulphuric Acid with or without* O_2^{2-} *Ligand,* to be published.

Paper III.

Zheng, L., Alstad, J., Bjørnstad, T., Polakova, D., Stavsetra, L., Omtvedt, J. P., *Studies on the Influence of KCl from SISAK Gas Jet on the Extraction of Rutherfordium Homologues from Sulphuric Acids with Tri-octylamine in Toluene with the SISAK System*, *Recent Advances in Actinide Science (Actinide 2005), The Royal Society of Chemistry*, ISBN -10: 0-85404-678-X.

Paper IV.

Omtvedt, J. P., Polakova, D., Alstad, J., Bjønstad, T., Düllmann,C., E. Folden III, C. M. Garcia, M. A. Gates, J.Gregorich, K. E. Hoffman, D. C., Nelson, S. L., Omtvedt, L., Pershina, V., Samadani, F., Skanemark, G., Stavsetra, L., Sudowe, R., Wilson, R.E., Zheng, L., Zielinski, P. M., *Liquid-liquid Extraction Studies of Rutherfordium-Sulphate Complexes by the SISAK System*, to be published.

1 Introduction

1.1 Transactinides

Chemical properties of an element depend on the element's electronic structure. The Periodic Table of the Elements illustrates recurring ("periodic") chemical properties. Rows are arranged so that elements with similar properties fall into the same vertical columns ("**groups**"). Each horizontal row ("**period**") in the table corresponds to the filling of a quantum shell of electrons. According to quantum mechanical theories of electron configuration within atoms, the progressively longer periods further down the table group the elements into **s-**, **p-**, **d-** and **f-blocks** to reflect their electron configuration. The main value of the Periodic Table of the Elements is that it enables one to predict the chemical properties of an element based on its location on the table [1-3]. After Glenn T. Seaborg introduced the actinide concept [4] the Periodic Table of the Elements was extended to include the then heaviest known elements. The addition of the the transactinide elements (TAEs) ($Z \geq 104$) [5, 6] or, as they are also called, superheavy elements (SHEs), has resulted in the modern periodic table, similar to that presented in Fig. 1.1. Presently, we know of 25 man-made transuranium elements. In 1997, IUPAC approved the names and chemical symbols of TAEs with Z = 104~109. In 2003–2004, the names and chemical symbols of elements 110 and 111 were approved. The remaining TAEs have no names so far. According to the actinide concept, the 5f electron series ends with element 103, lawrencium (Lr), and a new 6d transition series is predicted to begin with element 104, rutherfordium (Rf) [7]. The currently discovered 14 transactinide elements, with Z = 104 through 116 and 118 [8], are placed in the periodic table under their lighter homologues in

the 5d electron series, Hf to Hg, in the successive groups 13 to 16, and 18, Tl-Po and Rn (see Fig. 1.1).

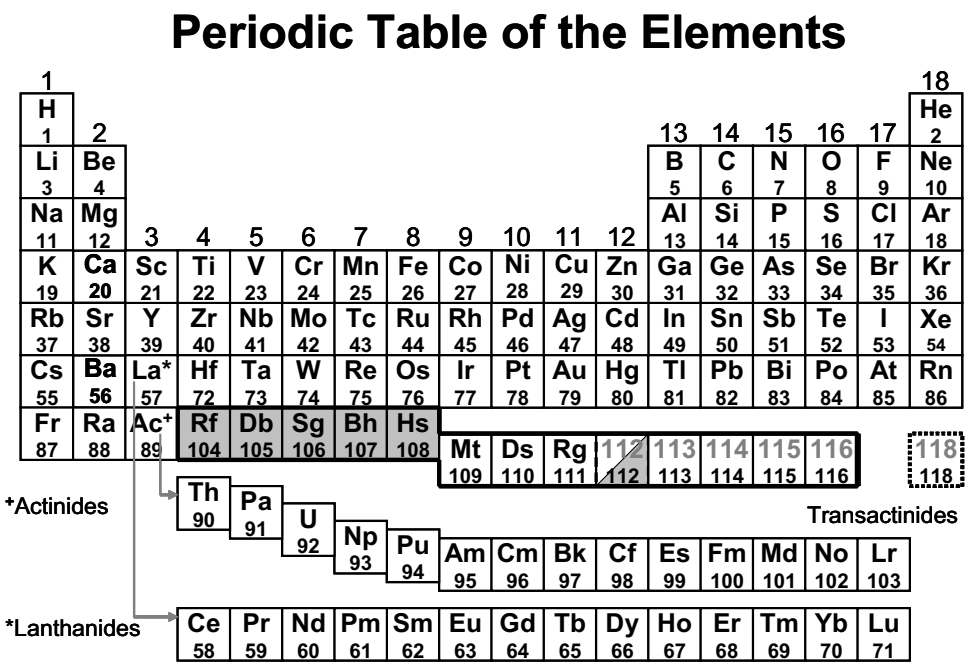

Fig. 1. 1 The Periodic Table of the Elements

For the TAEs, since the filling of the 6d-shell takes place, they are expected to exhibit chemical behaviour similar to that of the 4d and 5d transition elements. However, increasing deviations from the periodicity of chemical properties based on extrapolation from lighter homologues in the periodic table are predicted as the atomic number increases [9]. Electrons in orbitals with a high probability density near the nucleus are accelerated by the large nuclear charges to relativistic velocities, which increase their binding energies causing the orbital contraction and energetic stabilization of the s and $p_{1/2}$ shells. Furthermore, this leads to more efficient screening of the nuclear charge and corresponding radial expansion and energetic destabilization of the $p_{3/2}$, d and f orbitals. The relativistic effect also results in spin-orbit (SO) splitting of levels with $l > 0$ (p, d, f, … electrons) into $j = l \pm {}^1/_2$. These changes may lead to a different arrangement of the outermost orbitals compared to the one expected from extrapolations from the lighter homologues [9]. Therefore, changes not

expected from simple extrapolation of properties within a group of the periodic table might results. These relativistic effects increase approximately as a function of Z^2 and they are most pronounced in the heaviest elements [10]. Therefore, the heaviest elements provide a powerful testing ground for examining the influence of relativistic effects , this is an important reason why studies of the transactinide elements are of great interest [11]. For example, the stable oxidation states of a transactinide element might include unexpected valence states.

The TAEs spontaneously decay; the most stable of them have half-lives of only a few minutes. Many are much less stable and only exist for a small fraction of a second. For most known isotopes of the elements heavier than Z = 104, α-decay is the dominant decay mode instead of spontaneous fission. The half-lives of the isotopes of a given transactinide increase with increasing neutron number within the known region of TAEs [12-14]. A prominent α-decay mode of at least the mother and first daughter in the decay chain is necessary for an unambiguous determination and identification of isotopes of transactinide elements because a positive identification of a transactinide nuclei usually demands identification of a reasonable decay chain, e.g. correct mother and daughter α-energies and correlation time between them. Furthermore, for chemical investigations, half-lives of at least 1 s are necessary to allow enough time for the chemical apparatus to perform the required chemical operations [15]. Due to very short lifetimes and low production rates of TAEs, not only fast radiochemical separations and detection techniques need to be developed, but also facilities and expertise in preparation, irradiation, and handling of radioactive targets and subsequent separation of the desired nuclides from the complex reaction products are indispensable.

Suitable methods for chemical studies of TAEs are based on the principle of chromatographic separation either in the gas phase, by exploiting the differences in the volatility of TAE compounds, or in the aqueous phase by solvent extraction, or by ion-exchange separation using differences in their complex formation properties. Studies of the TAEs in the gas phase have been exploited quite a lot because they allow for the investigation of the TAEs with very short half-lives.

However, investigations in the gas phase are limited to volatile compounds. Solution chemistry provides another perspective for chemical studies of the transactinide elements. Properties such as complex formation can easily be investigated in the liquid phase. Model experiments on the isolation and investigation of TAEs in solutions by ion-exchange chromatography in the on-line mode demonstrated the possibility of studying the physiochemical properties of radionuclides with half-lives down to about 5–10 s. Short-lived radionuclides with half-lives of around 4 s were isolated and detected using the SISAK III (see 1.2) liquid-liquid solvent extraction system [11, 16, 17].

The short half-lives and very low production rates for the transactinide elements imply that each atom produced decays before a new atom is synthesized. For example, with hot fusion reaction applies to synthesize nuclides of elements 104 through 108, cross sections vary from about 10 nb to a few pb. With typical beam intensities of 3×10^{12} ions per second on targets of about 0.8 mg/cm^2 thickness production yields range from a few atoms per minute for rutherfordium and dubnium isotopes to five atoms per hour for ^{265}Sg and even less for ^{267}Bh and heavier nuclides. Such extreme conditions imply that any chemistry to be performed must be conducted on a "one-atom-at-a-time" basis [18, 19]. However, in macro-amount chemistry, the distribution ratio is defined as the concentration of all species of one element in the organic phase to the concentration in the aqueous phase. When a single atom is considered, the classical derivation of the law of mass action is no longer valid because a single atom cannot exist in two different phases simultaneously. Therefore, an expression equivalent to the law of the mass action has been derived, in which concentrations are replaced by probabilities of finding the atom in a given state and phase [20].

The first generation chemistry of the TAEs (mostly in gas phase), had concentrated on the question of how well the periodic table accommodates the transactinide elements as transition metals in the seventh period [20]. The second generation chemistry of the TAEs places stress on performing such experiments so as to enable detailed comparisons of the chemical properties of the TAEs to their lighter homologues or pseudohomologues, and compares the chemical properties of the TAEs with the properties deduced from extrapolations and from modern relativistic molecular orbital calculations [7]. Thus, for studying the chemical properties of the TAEs, the knowledge of the behaviour of their

homologues/pseudo-homologues under the same conditions is imperative. New methods are continuously being developed to advance the knowledge about the chemical properties of the TAE. Table 1.1 lists the isotopes of TAEs, chemically studied in solutions. These experiments were carried out in several research centres in the world [8].

Table 1. 1 Isotopes of transactinide elements studied by chemical methods in solutions

Isotope	T ½ (s)	Production reaction	Investigation method	Research centre (year)	Ref.
^{261}Rf	78	^{248}Cm(^{18}O,5n)	Ion-exchange chromatography	LBL (1970)	[21]
	″	″	″	FLNR JINR (1990)	[22]
	″	″	″	FLNR JINR (1998)	[23]
	″	″	″	PSI (2000)	[24]
	″	″	″	JAERI (2002)	[25]
	″	″	″	JAERI (2004)	[26]
	″	″	″	GSI (2004)	[27]
	″	″	Extraction chromatography	LBNL (1980)	[28]
	″	″	″	PSI (1998)	[29]
	″	″	Liquid-liquid extraction	LBNL (1994)	[30, 31]
	″	″	″	LBNL (1996)	[32, 33]
	″	″	Adsorption	LBNL (1996)	[34]
^{257}Rf	4.7	^{208}Pb(^{50}Ti,n)	SISAK on-line extraction	LBNL (2002)	[16]
^{257}Rf	″	^{208}Pb(^{50}Ti,n)	SISAK on-line extraction	LBNL (2003)	[17]
^{257}Rf	″	^{208}Pb(^{50}Ti,n)	SISAK on-line extraction	LBNL (2005)	[17]
^{262}Db	34	^{249}Bk(^{18}O,5n)	Adsorption, extraction	LBNL (1988)	[35]
	″	″	Extraction chromatography	LBNL (1989)	[36, 37]
	″	″	″	LBNL (1992)	[38]
	″	″	″	LBNL (1999)	[39]
^{263}Db	27	^{249}Bk(^{18}O,4n)	Ion-exchange chromatography	LBNL (1992)	[40]
		^{248}Cm(^{19}F,5n)	″	IN2P3-UPS (2002)	[41]
^{262}Db	27	^{249}Bk(^{18}O,4n)	″	GSI (2003)	[42]
	34	^{248}Cm(^{19}F,5n)	″	JAERI (2004)	
^{265}Sg	7.4	^{248}Cm(^{22}Ne,5n)	″	GSI (1997)	[43]
	″	^{248}Cm(^{22}Ne,5n)	″	GSI (1998)	[44]

Note: LBNL is Lawrence Berkeley Laboratory (Berkeley, USA), PSI is Pau Sherrer Institute (Villigen, Switzerland), JAERI is Japan Atomic Energy Research Institute (Tokai-Mura, Japan), GSI is Gesellshaft für Schwerionenforschung (Darmstadt, Germany), IN2P3-UPS is Institute de Physique Nucleaire, Radiochimie (Orsay, France), FLNR JINR is Flerov Laboratory of Nuclear Reactions, Joint Institute for Nuclear Research (Dubna, Russia).

1.2 SISAK

SISAK is an acronym for **S**hort-lived **I**sotopes **S**tudied by the **AK**UFVE technique, in which AKUFVE, a Swedish acronym, refers to arrangement for continuous investigations of distribution ratios in liquid-liquid extraction. The SISAK system was developed in the 1970s for chemical isolation of short-lived nuclides from complex nuclear reaction production mixtures [45]. Subsequently it has been used for investigating both chemical and nuclear properties of numerous elements and nuclides. Today, the third generation has been reached [46]. Based on the third generation of SISAK centrifuges, the SISAK 3, is a fully continuous multistage solvent extraction system. The most significant changes are the reduction of the hold-up volume and residence time of the apparatus. The previous SISAK 3 centrifuges were constructed of palladium-passivated titanium. The present centrifuge material is PEEK (Poly Ether Ether Ketone), which is used because it is more resistant to common acids such as hydrochloric and sulphuric acid [47, 48] and is therefore used presently.

During the last decade of the twentieth century, the system was adopted for transactinide research. A detection system based on liquid scintillation in combination with fast on-line liquid-liquid extraction using SISAK 3 was developed [49, 50] for detection and identification of nuclides through their α emission. It was compatible with the large flow rates of the SISAK apparatus, and could be designed to operate in a continuous manner. It turns out to be a practical method for studying the liquid chemistry of TAEs [51].

Early attempts to study transactinide nuclides with the SISAK system in the 1990s ended up with inconclusive results [6, 48, 52-56]. The main problem was the system's inability to distinguish α particles emitted from the desired TAE nuclide from the activity of transfer products because of the undesirable reactions between the projectile beam and target-backing material, aerosol particles and even carrier gas. The β- and γ-induced background from the surroundings and from nuclides produced in the target interfere with the α-spectrum analysis to such an extent that it becomes impractical [57].

In combination with a physical preseparator, for example, the Berkeley Gas-filled Separator (BGS), the SISAK Liquid-Scintillation experiments, using preseparated nuclei, profit from a strongly reduced background and more "chemistry-friendly" conditions. Chemical reactions can be performed without interference from intense heavy-ion beams and unwanted by-products. Thus, the chemistry can be optimized for studying the chemical properties of the TAE of interest without simultaneously functioning as an extremely efficient separation system. This gives more freedom in designing the chemical system used to investigate the chemical properties of the TAEs [17].

1.3 Objectives

The main objective of this work was to develop, using the SISAK system, suitable chemical separation systems and conditions for revealing the chemical behaviour of dubnium (Db, Z=105) in liquid phase relative to its homologues, niobium (Nb) and tantalum (Ta), and even its pseudohomologue, protactinium (Pa) with the SISAK system. The assumption made is that Db will behave in a similar manner to its homologues. In previous studies of Rf using SISAK, it proved feasible to use trioctyl amine (TOA) dissolved in toluene to extract Rf and its homologues, Zr and Hf [58] from sulphuric acid solutions. Using a procedure based on this extraction system, one was able to distinguish between zirconium-like and hafnium-like behaviour. This is an important first step in learning details about the chemical properties of a transactinide element. Based on the experience gained in studies of Rf using SISAK with TOA/H_2SO_4 to extract rutherfordium, similar extraction chemistry was chosen as starting point for the work. Furthermore, a different extracting agent, Aliquat 336, was investigated to expand the available experimental data on TOA's use in aqueous-phase dubnium complexes, which is important, for example, in theoretical calculations on types and stabilities of such complexes.

Due to the high amounts of liquid consumed by the SISAK system during transactinide experiments, which typically lasts several days, recycling of chemicals is necessary to reduce chemicals expense and waste products. This recycling results in build-up of KCl in the aqueous phase (from the KCl-aerosol particles used as carriers in the gas-jet), which

might have an influence on the extraction of the TAE of interest. Thus, it was necessary to check the possible influence of KCl for studies of the chemistry of the TAE.

2 Background

Dubnium and its horologues:

The element with atomic number 105 is the second transactinide element, dubnium (Db); it follows after element 104, rutherfordium (Rf). According to the systematics of the periodic table, Db should be located in Group 5, with Ta presumed to be its closest relative. Vanadium (V) and niobium (Nb) are also its homologues. Another element which in many ways behaves similarly to the Group 5 elements is protactinium (Pa), which therefore frequently is referred to as a pseudohomologue. The most stable oxidation state for Nb and Ta is +5 but both metals can be reduced to be in the +4 and +3 states; similar behaviour is thus expected for Db.

The expected ground state electronic configuration of Db is [Rn] $5f^{14}6d^{3}7s^{2}$.The ionization of Db in aqueous solutions is expected to stop with the [Rn] $5f^{14}$ core intact, leading to Db^{5+}, analogous to Ta^{5+} (with the [Xe] $4f^{14}$ configuration). The +5 oxidation state probably exists in aqueous solutions as a hydrolyzed or complexed species, such as, MO_2^{+} [35].

The aqueous chemistry of the Group-5 elements in the +5 state is well known (except for Db): Strong complexes can be formed with e.g. fluoride, chloride and sulphate ions. The Group-5 elements can also be efficiently extracted from a nitric acid medium using reagents like tributyl phosphate (TBP) or di-ethylhexyl-orthophosphoric acid (HDEHP).

The Group-5 elements, as well as Pa, form rather strong anionic or neutral complexes with hydroxy acids like glycolic acid, α-hydryoxyisobutyric acid and lactic acid [15].

2.1 Chemical Investigation of Dubnium

The first chemical studies of Db were performed by ZVÁRA et al. [59, 60] using gas-phase thermochromatography on the relatively volatile bromide and chloride complexes. The ^{243}Am (^{22}Ne, 4-5n) reaction was used to produce the nuclides of 2 s $^{261–260}$Db. In the experiments, the spontaneous fission (SF) track distribution along the thermochromatography column was assumed to characterize the element 105's behaviour. This distribution indicated that Db behaves like a typical transactinide element, that the chlorides and bromides of Db are less volatile than Nb compounds, and that Db compounds show a volatility which is rather similar to, or only slightly higher than the volatility observed for the Hf behaviour in Group 4. The authors of the experiment concluded that element 105 is a homologue of the Group-5 elements Nb and Ta. Their results were differently interpreted: either that Db behaves more like a Group-4 element or that its behaviour more closely resembles that of the tetrachloride of V or the oxychlorides of V and Nb [61, 62].

The first aqueous chemical experiment on Db was a study of the adsorption from an acid solution onto glass surfaces, which have been fumed twice with concentrated HCl and HNO_3 solutions [35]. The results show that Db in HNO_3 solution adheres with high yield to glass surfaces, a behaviour very characteristic of the Group-5 elements Nb and Ta, and of Pa. The other experiment was an attempt to study the extraction of Db fluoride complexes from a mixture of HNO_3 and HF into methyl isobutyl ketone (MIBK). The extraction of Nb and Ta from acidic fluoride solutions into MIBK is well known, and has been used as a very characteristic separation and purification process for these elements [58, 63, 64]. Ta extracts under a broader range of conditions than does Nb. If this Group-5 trend were to continue, Db should also form extractable species and be quantitatively extracted under the same conditions as Ta. However, it was found that Db did not form extractable anionic fluoride complexes [35]. Presumably the tendency to hydrolyze or to form high coordination number fluoride complexes in Db may be stronger than in Ta, leading to non-extractable species. Under such a condition, Nb was not extracted into the MIBK phase. The most obvious

explanation is that there occurs a formation of multi-charged anions such as $[DbF_7]^{2-}$. The higher charge would then prevent extraction into solvents, such as MIBK, with relatively high dielectric constant. The existence of a different valence state, like Db^{3+}, with a $[Rn]5f^{14}7s^2$ configuration due to the relativistic stabilization of the 7s electrons was also discussed [35]. However, on the basis of the calculations of Desclaux [65] it was not considered likely except under very strongly reducing conditions.

The first detailed comparisons of the chemical behaviour between Db, its lighter homologues Nb and Ta, and the pseudo-homologue Pa were carried out using solutions at different HCl concentrations with small amounts of HF added. They were performed as liquid-liquid extraction chromatography experiments with tri-iso-octyl amine (TIOA) as stationary phase on an inert support in the ARCA (Automatic Rapid Chemistry Apparatus) [36, 37] (see 3.3.2). In these experiments Db again showed a non-Ta-like behaviour and, even showed Pa-like properties.

The explanation of these results is hampered by the use of the mixed HCl/HF solution which did not allow to clearly distinguish which complex was formed. It was suggested that the non-tantalum-like halide complexation of Db is indicative of the formation of oxohalide or hydroxohalide complexes similar to $[NbOCl_4]^-$ and $[PaOCl_4]^-$ or $[Pa(OH)_2Cl_4]^-$, in contrast to the pure halide complexes of Ta, such as $[TaCl_6]^-$. In contrast to the experimentally observed extraction sequence from HCl solutions with small amounts of HF added, the inverse extraction order Pa >> Nb ≥ Db > Ta was predicted theoretically. This work considered the competition between hydrolysis and chloride complex formation. The subsequent experimental studies performed in the pure F^-, Cl^-, and Br^- system are in good agreement with the theoretical predictions which include relativistic effects [66, 67].

Extractions of Nb, Pa, and Db into di-isobutylcarbinol (DIBC) from concentrated HBr solutions showed that the tendency to form multi-charged anions is increasing in the sequence Pa<Nb<Db. Elutions from cation exchange columns with unbuffered 0.05 M α-hydroxi-isobutyric (α-HIB) solutions showed that Db, together with Nb and Ta, elutes promptly whereas tri- and tetravalent ions are strongly retained under these conditions. This provided an unambiguous proof that pentavalent Db is the most stable valence state in

aqueous solution, and it also supported the position of Db as a member of Group 5 of the Periodic Table [6, 38, 40].

In summary, pentavalent Db is the most stable valence state in aqueous solution. Most results show that Db has a non-Ta-like behaviour and in some conditions is even similar to Pa.The non-Ta-like behaviour of Db, and Db's similarity to Nb and /or Pa depend on its chemical environment. Therefore, the chemical properties of Db cannot be reliably extrapolated from the trends observed in its lighter homologues any more.

From the above, it is seen that so far most chemical studies of Db performed are about Db halide complexes whether in either gas or liquid phase. Very little has been exploited about Db sulphate/bisulphate complexes; in other words, the chemistry about Db sulphate/bisulphte complexes in solutions is greatly lacking.

2.2 Chemical Investigation of Superheavy Elements with SISAK

In the 1990s the Mainz-Gothenburg-Oslo SISAK collaboration started to develop plans for using the fast liquid-liquid extraction system SISAK for chemical studies of the transactinide elements. In his 1994 thesis, Pense Maskow proposed a liquid-liquid extraction scheme for use with SISAK for extraction of Group-4 elements [68]. The system was based on selective extraction from HNO_3 into dibutyl phosphoric acid (HDBP) in toluene, in which Hf and Zr were well separated from lanthanides and Group 5 and 6 elements (Nb, Ta, Mo, and W). In the following years work was performed to develop extraction systems for Rf, Db and element 106, seaborgium (Sg). Parallel to this work a liquid scintillation detection system was developed [49, 51, 69] to detect the α-decay of the transactinides. Liquid scintillation detection was selected as the only system which could handle the high volumes of liquid needed to operate the SISAK system. At GSI, PSI and LBNL several attempts to extract and detect Rf, Db, and Sg were made, but all with inconclusive results. A summary of these experiments can be found in Table 1.1 in the thesis of Stavsetra [70] and references therein. It should be noted that in all these experiments the product stream from the target was fed

directly (by use of a conventional aerosol-seeded gas-jet in a thin capillary) to the SISAK degasser. Thus, huge amounts of (unwanted) radioactivity were fed into the chemistry system. Even if only a small fraction of this were transferred to the organic phase, the beta background would practically blocked out any αs which might have entered the organic phase. This problem is especially severe for liquid scintillation detection, since β particles produced about ten times as much light as do α particles. Thus, the β spectrum resides in the same part of the spectrum as do the αs. Details about this are explained in Stavestra's thesis [70] and standard textbooks on α liquid scintillation spectroscopy, see e.g. the book by McDowell & McDowell [57].

In 2000, the Berkeley Gas-filled Separator (BGS) at Lawrence Berkeley National Laboratory (LBNL) was used as a physical preseparator between the transactinide producing target and SISAK. In this way nearly 100% of the unwanted activity was eliminated before it reached the chemistry apparatus. Therefore, the spectra contained only a relatively modest background (mostly from electrons created by a Compton interaction caused by outside γ rays entering the detection cells) and the α particles could relatively easily be identified in the spectrum (pulse shape discrimination is used to separate α and β particles). This was the first time a transactinide element was extracted and unequivocally identified by the SISAK system. Thus, it demonstrated that the fast liquid-liquid extraction system SISAK, in combination with liquid-scintillation detectors, could be used for investigating the chemical properties of the TAEs. It was also the first time a physical preseparator had been used in front of a chemistry system in a transactinide experiment and demonstrated the huge advantages of doing so – significantly reduced background activity.

In the 2000 SISAK experiment, only one step extraction was applied (see Fig. 3.2). Thus, the activity in the aqueous phase was not measured because water and acids destroy the energy resolution that is necessary for precise LS α spectroscopy [16]. Thus, to be able to calculate the distribution ratio between the two phases, the total amount of activity entering the system must be determined indirectly. This is achieved by running an experiment without extraction; all the activity is fed directly to the detectors, thus giving a measurement of the total amount of activity entering the chemistry system. The measured activity in the organic phase is then subtracted from the total activity. The difference is then assumed to be the amount of activity in the aqueous phase. Since the two experiments cannot be performed simultaneously, the beam integral (from e.g. Rutherford scattering detectors, as used at the BGS) is used for normalisation. However, this procedure assumes that the transport

efficiency throughout the complete system is constant, something which is only partially true for the gas-jet transfer.

3 Methods and Instrumentation

3.1 Production of Transactinides

Transuranium elements are usually synthesised in high neutron-flux reactors in which the elements are formed from a chain of neutron captures and subsequent β-decays. With this method, neutron rich isotopes of elements up to fermium (Z = 100) can be produced. At fermium, however, the method's utility ends due to the lack of β- decay and too short α and fission half-lives of the heavier elements. The elements beyond fermium are most accessible using heavy-ion fusion reactions. This is achieved by bombardment of heavy-element targets with heavy ions from an accelerator. As the neutron excess increases for heavy nuclei, heavy-ion reactions lead to neutron deficient and unstable species. This can, to some extent, be compensated by the use of neutron rich targets and projectiles.

There are mainly two types of fusion reactions, hot and cold. Hot fusion reactions are based on targets made from actinide elements such as ^{248}Cm, ^{249}Bk or ^{249}Cf with a light projectile. Depending on the TAE to be produced, ^{18}O or ^{22}Ne can be used as the projectile. A cold fusion reaction is, for instance, based on lead and bismuth targets and the projectile can be ^{50}Ti, ^{54}Cr or ^{58}Fe. The most significant difference between the hot and cold fusions is that the excitation energy of the compound nucleus is at the lowest beam energies necessary to initiate a fusion reaction. Values are at 10–20 MeV in reactions with lead targets and at 35–45 MeV in reaction with actinide targets. The second important difference is that the

actinide target-based reactions in hot fusion produce more neutron-rich isotopes of the same element than a cold fusion reaction does, e.g. ^{269}Hs from a ^{248}Cm target and ^{264}Hs from a ^{208}Pb target [20]. Unlike in the sequential neutron capture process, in the fusion process, the total mass of the projectile is imported into the target nucleus. The fusion of complex nuclei leads to an excited compound nucleus. Its transition to the ground state is achieved by means of neutron- and γ-ray emission. Fission strongly competes with this process. As a result, the survival probability of the nucleus strongly decreases. The evaporation of a neutron reduces the excitation energy by about 10 MeV, which means that several steps of neutron evaporation may be needed before the "final" product is formed. Since the excitation energy is lower for the compound nucleus formed in cold fusion compared to the one formed in hot fusion fewer neutrons have to be evaporated to dissipate the excitation energy. Thus, cold fusion reactions tend to give the largest cross sections for production of transactinide nuclides. However, the nuclides formed in cold fusion reactions have fewer neutrons than those formed in hot fusion reactions. The former usually yields a shorter half-life of the product [71]. Production reactions of some transactinides used for chemical research are listed in Table 3.1.

For SISAK on-line experiments concerning transactinides, the main facilities are composed of three parts:

- The target chamber , preseparator (e.g. BGS) and transportation system of reaction products
- Chemical separation system
- On-line detection system

Relating to production of transactinide nuclides, the target chamber is the main facility.

Target Chamber

The construction of the target chamber depends on the type of nuclear reaction used. Cooling of the target is provided by a gas stream, and the beam stop is normally water-cooled. One type of such a target chamber is illustrated as Fig. 3.1. At the Oslo cyclotron lab (OCL) the beam energy used is relatively low and the energy dissipation correspondingly low. Hence, additional cooling systems are unnecessary and therefore the target chamber construction is comparatively simpler as shown in Fig. 3.2. The MC35 Scanditronix Cyclotron of the OCL can deliver beams of several particle types such as

protons (E_{pmax} = 35 MeV), deuterons (E_{dmax} = 18 MeV), ^{3}He (E_{3Hemax} = 47 MeV) and ^{4}He (E_{4Hemax} = 35 MeV), see Table 3.2.

Table 3. 1 List of some production reactions of transactinides **[71]**

Reaction	Cross Section	Half-lives of product	Decay mode
$^{207}Pb(^{50}Ti, 2n)^{255}Rf$	4.8 ± 0.4 nb [72]	1.64 s [73]	α and SF
$^{208}Pb(^{50}Ti, 1n)^{257}Rf$	10 ± 1 nb [74]	3.9 s/4.0 s [73]	α and EC
$^{249}Cf(^{12}C, 4n)^{257}Rf$	10 nb [75] 12 nb [76]	3.9 s/4.0 s [73]	
$^{248}Cm(^{18}O, 5n)^{261}Rf$	5 nb [77]	78(+11,-6) s [32]	α
$^{209}Bi(^{50}Ti, 1n)^{258}Db$	2.9 ± 0.3 nb [78]	4.4 (+0.9,-0.6) s [78]	α and EC
$^{250}Cf(^{15}N, 5n)^{261}Db$	0.51 ± 0.20 nb [79]	1.8 (± 0.6) s [80]	α and SF
$^{249}Bk(^{18}O, 5n)^{262}Db$	6 ± 3 nb [81]	34 s [82]	α and SF
$^{249}Bk(^{18}O, 4n)^{263}Db$	10 ± 6 nb [81]	27(+10,-7) s [81]	α and SF
$^{248}Cm(^{22}Ne, 5n)^{265}Sg$	0.26 nb [83, 84]	7.4 (+3.3,-2.7) s [85]	α
$^{248}Cm(^{22}Ne, 4n)^{266}Sg$	0.08 nb [83, 84]	21 (+20,-12) s [85]	α
$^{249}Bk(^{22}Ne, 4n)^{267}Bh$	58 (+33, -15) pb [86]	17 (+14, -6) s [86]	α
$^{248}Cm(^{26}Mg,5n)^{269}Hs$	6 pb	9.3 s [87]	α

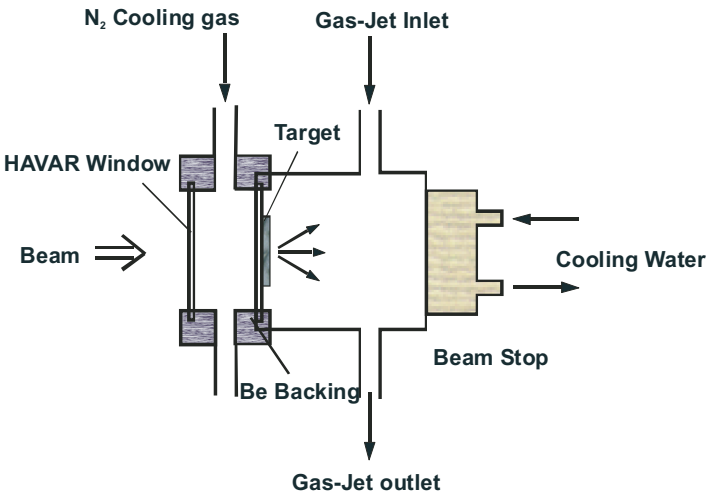

Fig. 3. 1 Schematic drawing of a typical target chamber with cooling gas at the target and cooling water at the beam stop

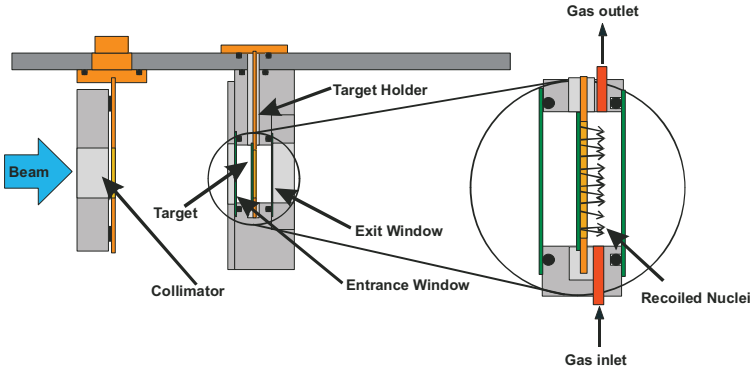

Fig. 3. 2 Schematic drawing of the OCL target chamber

Table 3. 2 Available Beams from the MC-35 Scanditronix cyclotron at OCL

Particle type	Energy (MeV)	Beam Intensity (μA)
Proton	2–35	100
Deuteron	4–18	100
^{3}He	6–47	50
^{4}He	8–35	50

3.2 Preseparation and Transportation of Nuclear Reaction Products

3.2.1 Physical Preseparator BGS and the Recoil Transfer Chamber (RTC)

Among the difficulties involved in identifying and studying the heaviest elements, besides increasingly short half-lives and very low production rates, are the overwhelming quantities of unwanted nuclides which are co-produced. Very special techniques are needed to separate the desired nuclides from the complex reaction products. Both physical and radiochemical separation techniques are used. The Berkeley Gas-filled Separator (BGS) employs a physical preseparation techniques, which uses the different magnetic rigidities of the recoils and projectiles travelling through a low-pressure, gas-filled volume in a magnetic dipole field. Helium is used in order to obtain a maximum difference in the rigidities of slow reaction

products and fast projectiles.

The BGS, consisting of quadrupole, gradient-field, and flat-field magnets, which can be coupled with the SISAK chemical separation system, was used as an efficient radionuclide separator at the Lawrence Berkeley National Laboratory [16]. The use of preseparated isotopes resulted in nearly background-free experiments which enabled unambiguous identification of TAEs, e.g., ^{257}Rf ($T_{1/2}$ = 4.3 s); details of this experiment were described by Omtvedt in an article [16]. Using the BGS preseparator enables direct measurement of the amount of TAEs entering the chemical separation system. Especially, for the one-step extraction with SISAK TAE experiments, this is important since the activity in the aqueous phase is not possible to measure with the liquid scintillation technique used. To calculate extraction yields, and thereby derive the D-values, the amount of TAEs entering the chemistry system is needed.

A multiple-target system is located inside the BGS, consisting of a 35 cm target wheel of nine arc-shaped target areas. The target wheel is located 0.5 cm downstream of the carbon (40μg/cm^2) entrance window of the separator, and rotates at 300 rpm. Two silicon p-i-n detectors mounted ± 27 degrees incident to the beam, measure elastically scattered beam particles. The separator is filled with He gas to a pressure of 70 ~ 130 Pa, and the beam particles and transfer products are spatially separated in flight from the evaporation residues (EVRs) and the desired nuclides pass through a 6-μm MYLAR foil and then are stopped in a volume of He at a pressure of 2 bar in the Recoil Transfer Chamber (RTC). In the RTC, where the He gas is seeded with KCl particles the TAEs nuclides become attached to the He/KCl aerosols and are sucked through a 20-m capillary to the chemical separation system. The transportation efficiency of the BGS is about 60% for the production of ^{257}Rf [70]. A schematic drawing of BGS is shown in Fig. 3.3.

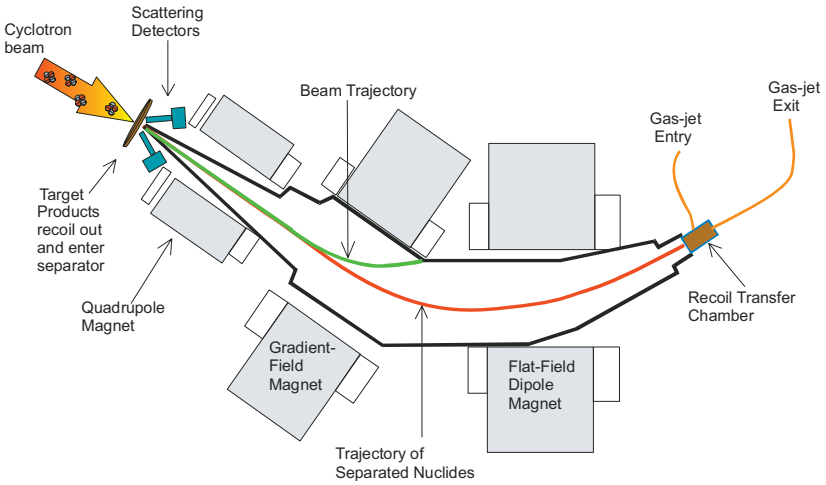

Fig. 3. 3 Schematic drawing of the target chamber and the BGS coupled to the RTC at the 88-inch Cyclotron at LBNL. A helium gas-jet system transports the recoils to the chemical separation area

3.2.2 Gas-jet

An efficient, fast and reliable transport of recoiling EVRs from target chamber to various chemical separation devices is a prerequisite for heavy-element research with chemical techniques. To achieve faster chemical separation times, the aerosol gas-jet transport technique has been used. The principles behind the aerosol gas-jet transport technique have been presented by H.Wollnik [88]. In the gas-jet recoil transport technique, products of nuclear reaction recoil out of a thin target and stop in a carrier gas, usually helium, at a pressure normally above 1 bar in a target chamber. The helium gas is seeded with aerosol particles. After stopping in the gas, the reaction products become attached to the aerosol particles. The activity-laden aerosol carried with the gas is sucked with the gas through a thin capillary tube to a remote site by applying vacuum to the downstream end of the capillary. Many aerosol materials, e.g. KF, KCl, KBr, NaCl and NaBr have been tested, and the aerosol material can be specifically chosen to minimize interference with the chemical separation being performed. Widely used are KCl aerosols which can easily be generated by sublimation of KCl from a porcelain boat within a tube furnace. By heating

KCl salt to about 650–670 ºC, aerosols with a mean mobility diameter of about 100 nm and number concentrations of few times 10^6 particles/cm^3 could be generated. Also $PbCl_2$ [89], graphite [90] and MoO_3 [32, 91] aerosols of about 50 to 200 nm size have been used with good results. Examples of such gas-jet systems applied in combination with a chemical separation system for TAE investigations are the SISAK system based on solvent extraction, the on-line gas chromatography systems for volatile species OLGA (**O**n-**L**ine **G**as Chromatography **A**pparatus) (see 3.3. 1), and the rapid batch-wise working system ARCA (**A**utomatic **R**apid **C**hemistry **A**pparatus) for liquid chemistry (see 3.3. 2).

As a continuous transportation technique, the gas-jet technique is easily coupled to systems for on-line chemicals separation and measurement experiments [92, 93].

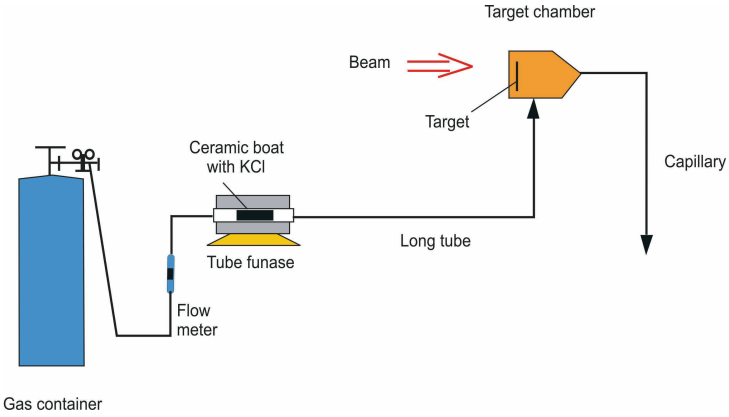

Fig. 3. 4 Schematic drawing of the gas-jet recoil transportation system at OCL

The combination of a gas-jet technique with the SISAK system was first reported by Trautmann et al. in an experiment isolating short-lived isotopes of cerium, lanthanum and praseodymium from a fission product mixture using ethylene/nitrogen as cluster/carrier gas [92].

With respect to the OCL gas-jet system the helium gas is fed from a gas container through a quartz tube containing a ceramic boat laden with potassium chloride. The quartz tube is placed in a tube furnace and kept at a temperature of around 670 ºC. The gas leaving

the quartz tube, with ACL aerosols, is then sucked through a tube section acting as a filter in order to remove small particles by collision with the tube wall as well as large particles by sedimentation. Large particles are also removed by a glass frit before the gas is fed into the target chamber [15]. A schematic drawing of the gas-jet transport system is shown in Fig. 3.4.

3.3 Instrumentation of Transactinide Chemistry

The instrumentation used for studies of transactinide chemistry is either on-line working or in a batch-wise mode. The chemical separation systems for transactinides are mainly based on gas phase separation and aqueous phase separation.

3.3.1 Gas-phase System

Pioneering chemical studies of volatile Rf, Db and Sg halids and /or oxyhalides [20] were carried out by gas chromatography. However, investigation in the gas phase is limited to volatile compounds. Also some disadvantages appear such as modest chemical separation factors and a rather limited number of volatile species that are suited for gas chromatographic investigation.

Since the synthesis of transactinide nuclei usually implies a thermalization of the reaction products in a gas volume, a recoil chamber can be connected with a capillary directly to a gas chromatographic system. Gas-phase separation procedures are fast, efficient and can be performed continuously, which is highly desirable in order to achieve high overall yields. For the experimental investigation of volatile transactinide compounds two different types of chromatographic separations have been developed, thermochromatography and isothermal chromatography. In thermochromatography [94] , a carrier gas flows through a chromatography column in which a negative temperature gradient is applied. Volatile species are deposited in the column according to their degree of volatility. By inserting

spontaneous-fission (SF) track detectors into the column, SF decays of short- and long-lived nuclides can be registered throughout the duration of the experiment.

In the isothermal gas-chromatography method, a carrier gas flows through a chromatography column of constant, isothermal temperature. At a certain temperature of the column, the retention time through the column is equal to the half-life of the introduced nuclide. The half-life of the nuclide is thus used as an internal clock for the system.

One of the most successful isothermal chromatography approaches to the study of transactinide is the **OLGA** (**O**n-**L**ine **G**as Chromatography **A**pparatus) technique, which allows the α-spectrometric measurement of the final products [9, 95-97]. To improve the chromatographic resolution and increase the speed of separation, OLGA (III) was developed. Time needed from separation to detection is for OLGA II about 20s and for OLGA III only a few seconds. A schematic drawing of OLGA (III) connected to either a rotating wheel or a tape detection system is shown in Fig. 3.5.

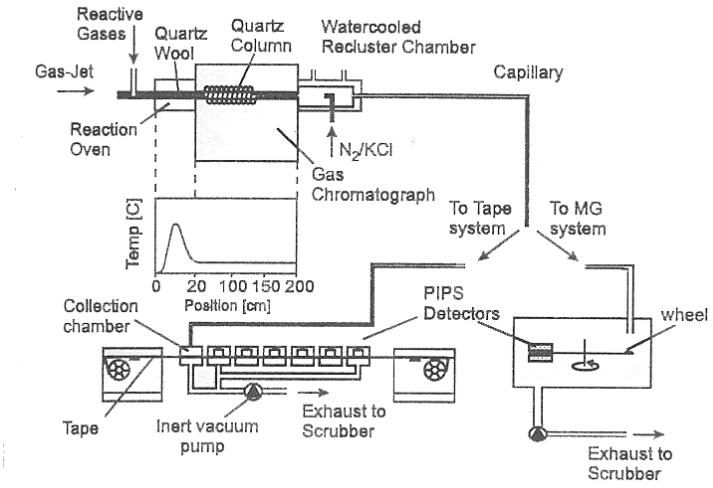

Fig. 3. 5 Schematic drawing and the principle of the method for on-line isothermal gas chromatography. Reprinted from [20].

The aerosols carrying the reaction products are collected on quartz wool inside a reaction oven. Reactive gases, halogenating agents, e.g. HBr, HCl or Cl_2, are introduced to form volatile species, which are transported downstream by the carrier gas flow to an adjoining isothermal section of the column, where the chromatographic separation takes place. The products leaving the column are reattached to clusters in the recluster chamber

and transported to the detection system, which can be based on a rotating wheel or a tape detection system. The wheel or the tape is moved between pairs of PIPs (Passivated Ions-implanted Planar Silicon) detectors providing α energy resolutions in the order of 20~30 keV [98, 99].

3.3.2 Aqueous-phase Systems

ARCA

The computer-controlled **ARCA II** (**A**utomatic **R**apid **C**hemistry **A**pparatus) is a chemically inert automated micro high performance liquid chromatography system [100]. Several chemical solution studies of dubnium were carried out by the ARCA II experimental set-up [37, 38, 40, 101]. ARCA II is composed of three main sections: a central integrated unit for collecting activity from the gas-jet and for performing the chemical separations, a section for transporting and storing the liquids containing pumps, valves and solvent reservoirs and an eletropneumatic valve system and a control unit with microprocessor. The main chemical separation section is shown in Fig. 3.6.

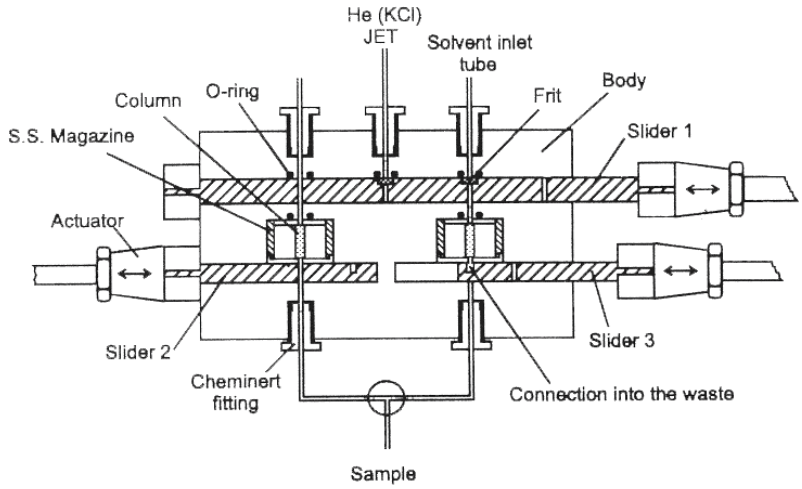

Fig. 3. 6 The general principle of the main chemical separation section of ARCA II. Reprinted from [20]

This system is symmetrical. While previously collected activity is dissolved and transported to a column for chemical separation on one side, meanwhile the activity from the gas-jet is collected on a polyethylene frit, and the next column is washed and conditioned on the other side. All parts in contact with the solutions are of inert materials such as

polyethylene, Kel-F, Teflon or sapphire, which resists mineral acids. The nuclides of interest are eluted from the columns onto heated tantalum or titanium plates. The eluent is evaporated by heating with an infrared lamp and heated gas stream. After cooling the tantalum or titanium plate is measured using a surface barrier detector. It takes typically 50 seconds from the end of irradiation to the start of measurements.

RACHEL

Another liquid separation system is RACHEL [41, 102-104] (**R**apid **A**queous **C**hemistry Apparatus for **H**eavy **El**ements). It is a system for continuous separation with three ion exchange columns. In this system the reaction products transported to a dissolver-degasser unit are dissolved in an aqueous medium and further transported into a series of cationic and anionic ion exchanger columns. In the first cation exchange column, of the reaction products the actinides and lanthanides are strongly captured. The studied transactinide, e.g. Rf or Db, is adsorbed on the following anion exchange column and the α-decay products from Rf or Db are kept on the third anion exchange column. After the columns were taken apart their activity of long-lived granddaughters ^{253}Fm and ^{253} Es is eluted and measured; thus, the adsorption behaviour of the nuclides of interest can be determined.

The three-column technique was used for the study of the chemical properties of Db using 34 s ^{262}Db, which was produced in the ^{248}Cm(19F, 5n)^{262}Db reaction and transported to the chemical separation apparatus with an aerosol gas-jet. The activities delivered by the gas-jet were continuously dissolved in an appropriate aqueous solution and passed through a series of three ion exchange columns. The first column was used to separate all of the directly-produced daughter activities, allowing the Db atoms to pass through to the second column, where they are quantitatively retained. As the Db atoms decay to Lr, Md, and Fm (via α- and EC-decay), they are desorbed from the second column and pass to the third column. The third column quantitatively retains the longer-lived daughter activities. Since all directly-produced Lr, Md, and Fm activities were retained on the first column, this third

column should contain only Lr, Md, and Fm atoms that are the decay descendents of Db atoms which were retained on the second column. At the end of a suitable production and chemical separation cycle, the daughter activities are chemically separated from this third column, and assayed for the α-decay of the ^{254}Fm great-granddaughter of ^{262}Db [20].

3.3.3 SISAK System

Being a fully continuous multistage solvent-extraction system based on H centrifuges [46, 105, 106], the SISAK III system has been developed for transactinide research. The main components or core parts of the system are the degasser and the centrifuges, the gas/liquid mixers and the liquid/liquid mixers, and the detection equipment. Chemical procedures used in the transactinide research are shown in Fig. 3.7, Fig. 3.8 and Fig. 3.9 respectively. Setup A is intended for direct measurement of the amount of activity entering the system. Setup B is constructed as a one-extraction-step for measurement of the amount of activity in the organic phase after extraction. Setups A and B are used together to enable calculation of the amount of activity in the aqueous phase in order to calculate distribution ratio values (D-values). Setup C, with a two-extraction-step system, is a more advanced procedure in which the activity in the aqueous phase after the first extraction stage is partially or completely extracted into the second organic phase. Thus, the activity in the two phases can be measured simultaneously, which simplifies the calculation of the D-values. The experimental techniques are under constant development and optimization to meet new requirements imposed by the research in the transactinide field. The general principles, technique, equipment and limitations are discussed in [15].

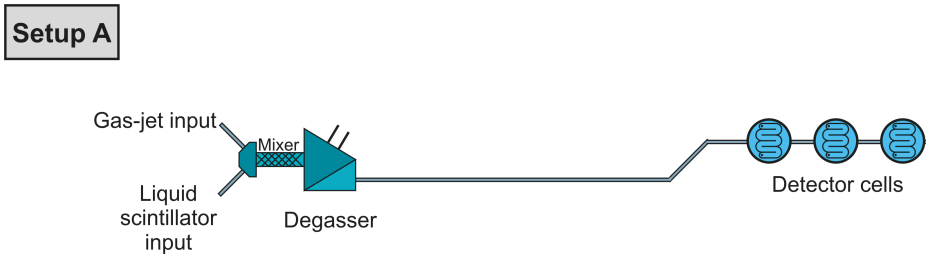

Fig. 3. 7 Setup for direct measurement of the amount of activity entering the system

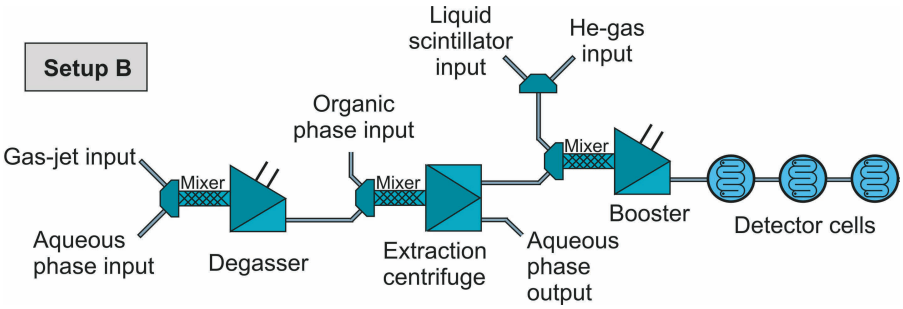

Fig. 3. 8 Setup with one-extraction step for measurement of activity in the organic phase

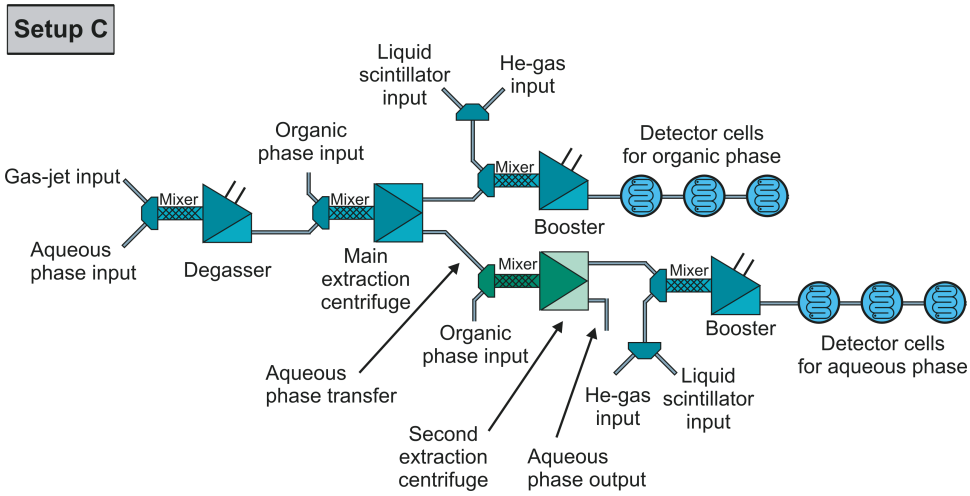

Fig. 3. 9 Setup with a two-extraction step for measurement of activity both in the organic and aqueous phases

Gas/liquid and Liquid/liquid Mixers

The species produced in the nuclear reactions have to be transferred from gas phase into liquid phase. Hence, a gas/liquid mixer is needed. There are two types of gas/liquid mixers, A and B, as shown in Fig. 3.10. Mixer A is a quartz tube with two glass frits inside where the mixing of gas and liquid takes place. The hold-up volume is about 2.6 ml. Mixer B is a zigzag-mixer. It consists of a PEEK rod with carved tracks, wrapped in a tube of quartz or PEEK. Along the crossings of these tracks the mixing of gas and liquid occurs. Two lengths of this mixer, 45 mm and 85 mm are produced. The efficiency of mixing He-jet transported radionuclides (0.5 L/min) into an organic liquid (0.4 ml/s) is in the range of 30% ~ 40% for

the two mixers at room temperature. When the radionuclides are dissolved in aqueous HNO_3 or H_2SO_4 solutions, the mixer efficiencies are typically between 67% ~ 86%. The number is a function of the flow rates of the liquid and gas-jet and the temperature of the aqueous solution. The highest efficiencies can be obtained at around 80 C° [70, 71].

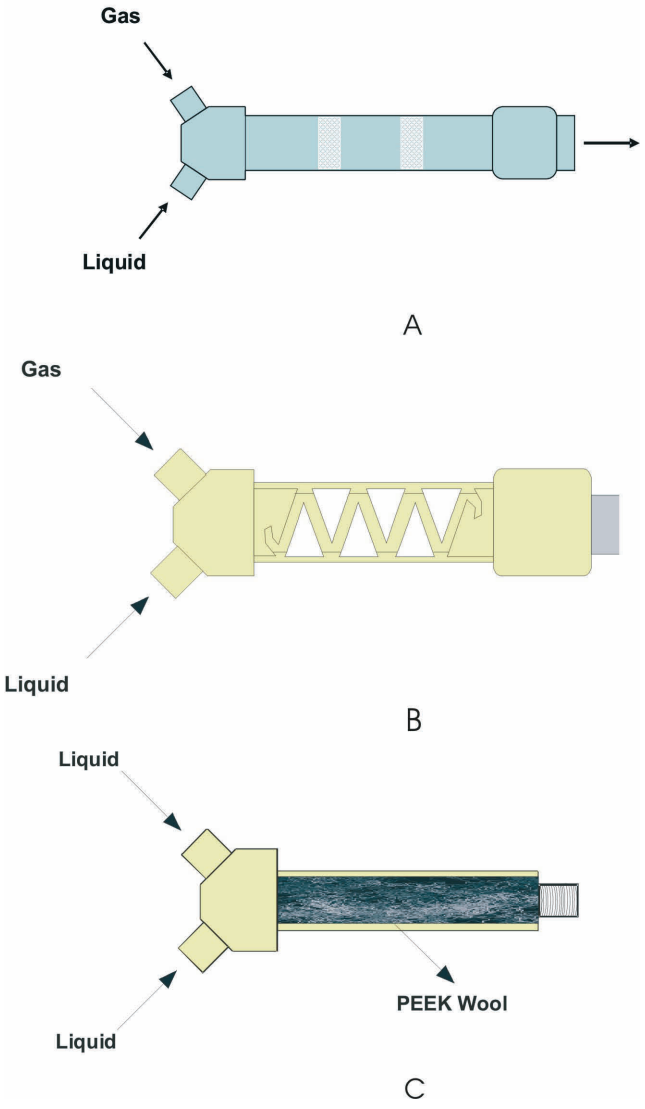

Fig. 3. 10 Schematic drawings of three different mixers. A and B are two types of gas/liquid mixers. C is a liquid/liquid mixer

Another construction is the liquid/liquid mixer as shown in Fig. 3.10 C. The purpose of using the mixer is to ensure that the aqueous phase and organic phase are mixed sufficiently

well to achieve a high extraction yield before the phases are separated in the succeeding centrifuge. Earlier SISAK setups only used a Y connector at this stage. The interior of the mixers is stuffed with PEEK wool.

The contact time of the two liquids depends on the mixer length used. By applying different lengths of the static mixer, while keeping other parameters constant, it is possible to measure the effect of the contact time on the extraction efficiency. The effectiveness of this type of mixer is determined by the diameter of the PEEK fibres and the compactness of the PEEK stuffing.

Degasser

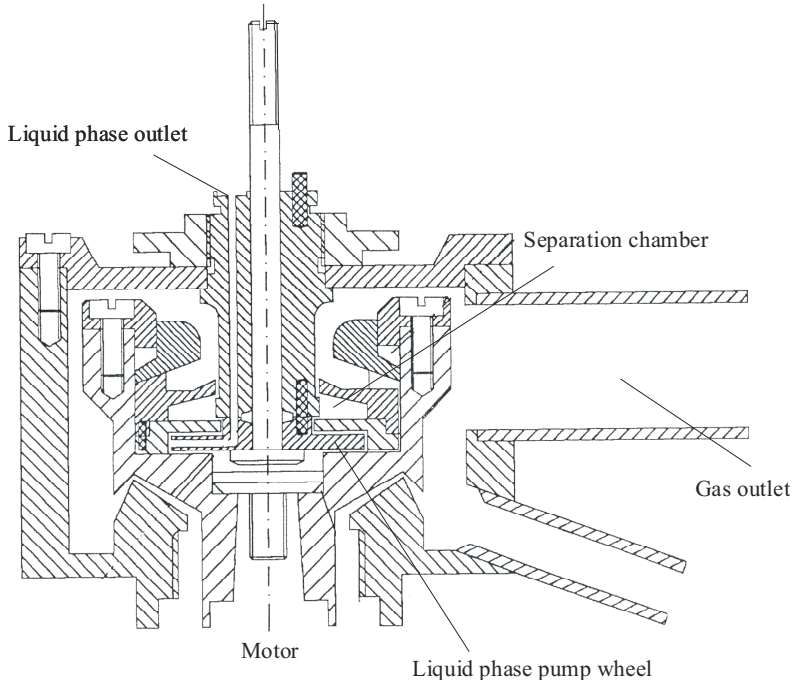

Fig. 3. 11 Cut-away drawing of the HG-0.1 degasser centrifuge. The gas and liquid mixture enters the separation chamber from the centre. Then, the gas moves up and exits through an opening in the outer wall. The liquid is forced downwards, and is pumped out of the centrifuge with a pump wheel.

Fig. 3.11. shows a cut-away drawing of the H-0.1 degasser centrifuge. The mixture of gas and liquid leaving the gas/liquid mixer enters centrally and is accelerated to the rotational speed within the inlet chamber. After acceleration the mixture is forced through three holes upwards into the separation volume, which contains three chambers. In each of these chambers the liquid is forced along the wall and then downward into the liquid phase collecting chamber where it encounters a stationary pump wheel conducting the liquid out of the degasser via a throttle valve. The valve guarantees a proper pressure balance in the degasser centrifuge so that gas bubbles do not escape through the liquid phase outlet. The gas is discharged through an outlet surrounding the central shaft and then fed into the exhaust system [46].

Liquid/liquid Centrifuge

The cut-away drawing of the H-0.3 centrifuge is illustrated in Fig.3.12. The mixture of the two liquid phases enters centrally the 0.3 centrifuge and is accelerated to the speed of rotation within the inlet chamber. After acceleration, the mixture is forced into the separation volume which contains four small chambers, symmetrically arranged around the axis of rotation and totally isolated from each other. In these separation chambers the mixture has to follow a zigzag motion imposed by the peripheral partition walls and interspersed baffle ridges. The separated phases are discharged - the light phase from the upper collecting chamber, the heavy phase from the lower one - by stationary pump wheels which are individually designed to provide the appropriate pressure and avoid excessive frothing of the liquids. The outlets are equipped with valves the purpose of which is to maintain a proper pressure balance in the centrifuge. By means of the valves the liquid-liquid interface can be adjusted such that both outgoing phases are free from entrainments of the opposite phase [46].

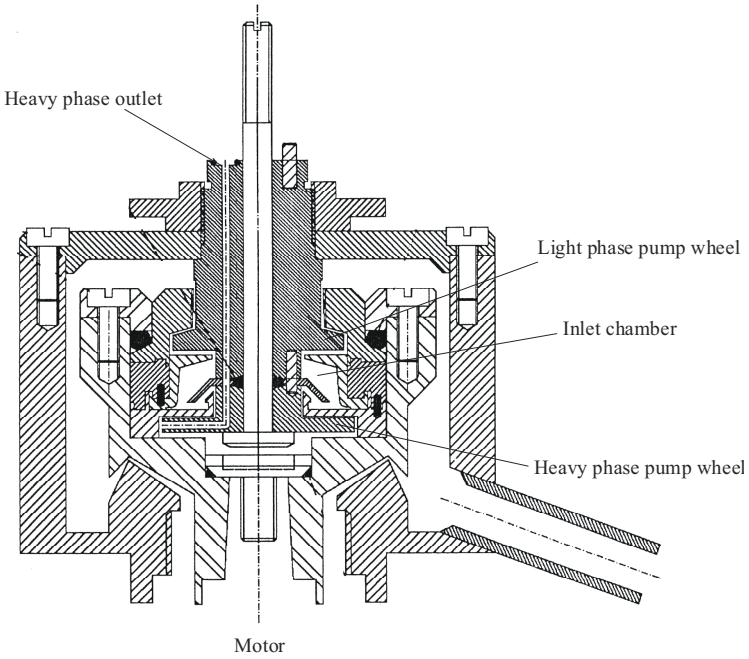

Fig. 3. 12 Cut-away drawing of the HG-0.3 centrifuge. The liquids enter the separation chamber from the centre. The phases are separated due to different centrifugal forces and each phase is discharged via a stationary pump wheel.

Pumps

Cog-wheel pumps with a flow capacity that can be continuously varied are used in the SISAK equipments as feed pumps. The flow rates of the pumps are measured with mass flow meters, and variation from the desired amount is controlled and adjusted by an automatic control system.

Detection System

i. Liquid Scintillation

The detection system for the on-line SISAK solvent extraction system used in TAE studies is based on liquid scintillation counting LSC. Liquid scintillation involves the conversion of the energy of a radioactive decay event into photons of light in a fluor (the light emitting molecules) solution with an organic solvent. The basic principle involved in this process is the excitation of scintillator molecules (fluor) by the transfer of energy from radioactive decay and deexcitation of the fluor molecules by emission of light. In photomultiplier tubes (PM-tube) coupled to a liquid scintillation detector this light is converted into an electronic

pulse and amplified. The amplitude of the pulse is proportional to the amount of light striking the photocathode of the PM-tube. α radiation, β radiation and low-energy gamma radiation are normally completely stopped in a scintillation solution. And the light output produced by the scintillator is proportional to the energy involved in the decay for a certain type of radiation. After energy calibration LSC can be used for α (or β) spectroscopy. A measurement system based on the combination of the liquid scintillation detection technique and fast, continuous on-line liquid-liquid extraction using SISAK 3 has been developed [51]. In this system, liquid scintillation detection can be applied on-line directly on the outgoing organic phase. Moreover, 4л measuring geometry inherent in the detection technique offers a nearly 100% detection efficiency for α and SF events, which is important concerning the low production rates of TAEs. However, liquid scintillation detection suffers from relatively poor α peak resolution. It is also sensitive to high β/γ count rates producing pile-up events interfering in the TAEs α decay energy region [49].

The most important techniques implemented are [16]:

1. Electronic pulse-shape discrimination is used to reduce the β/γ background in the α spectra by a factor > 1000. Without this technique the β- and γ-induced background from the surroundings and from nuclides produced in the target will interfere with the α spectrum to such extent that it becomes useless.
2. Real-time scintillation-yield monitoring by continuous measurement of the Compton edge of 662-keV ^{137}Cs γ rays is applied. The position of the Compton edge is used to automatically adjust the energy calibration. Based on this adjustment the event gates used for switching the detection cells between mother and daughter mode (open or closed valve, respectively) will always be set to the correct energy range.
3. Adding the scintillator chemicals after the final extraction step and flushing the mixture with an inert gas (Ar or N_2) to remove O_2. Oxygen quenches the scintillation processes; in particular, the time resolution necessary for the pulse-shape discrimination is severely affected. This procedure also improves the phase separation and extraction

yield. It is desirable to dry the sparging gas and saturate it with the solvent used in the scintillation, such as toluene, p-xylene, or others, before it is passed through the sample so that sparging will not evaporate solvent from the sample.

The energy loss per unit length of absorber depends strongly on the type of radiation. The heavy and highly charged particles lose more energy in the same length of absorber and the ionisation track will become denser. The dense ionisation track increases the probability of recombination reactions and ion-molecular interactions. The process of energy transfer from the ionised and highly excited molecules around a dense ionisation track is slower since these molecules must diffuse to find a pertinent molecule on which to deposit their excess energy. These effects result in a longer and smaller light output from an α or a spontaneous fission event than from a β or a γ decay. Alpha energy is only about one-tenth as efficient in producing light in a liquid scintillation system as beta and gamma radiation, e.g., a 5 MeV α particle has approximately the same scintillation light output as a 0.5 MeV β particle. This effect is very troublesome in alpha spectrometry by liquid scintillation since it means that alpha peaks will almost always be overlapped by a beta-gamma continuum. Thus, it is necessary to eliminate contamination of β- and γ-activity interference in an alpha spectrometry as much as possible. Fortunately, the time required for energy discharge for an α-event is much longer than for a β event or γ event, in other words, the α pulse diminishes and returns to zero more slowly than the β- or γ-produced pulse. These different timing characteristics of α and β events allows alpha-particle-produced pulses to be electronically discriminated from beta-and gamma-produced pulses in an α measurement, which can be achieved by measuring the difference in decay time between an α and a β pulse [57]. By setting proper gates in the timing spectra it is possible to discriminate β/γ and α events by such a pulse shape discrimination (PSD). With the PSD technique, one can expect to reject better than 99.95% of all beta and gamma pulses without loss of any alpha pulses. If two β particles are emitted close in time these may be treated as single α particle by the detection system, a ββ-pileup rejection system (PUR) has been constructed in order to reduce the pileup problem [51, 71].

Three component scintillation mixtures are normally applied in an α-liquid scintillation spectroscopy. Using a toluene-based extractive scintillator with naphthalene (primary scintillator) and dimethy-POPOP (secondary scintillator) has been adapted for the SISAK liquid-scintillation detection system [70]. In the SISAK detection system, the scintillation-light yield was enhanced by adding the scintillation solution to the organic exit-phase after the extraction. It was further improved when the gas-wash (booster) step was implemented, and naphthalene was substituted with 1-methyl naphthalene, a derivate more

soluble in toluene. A gas-wash step between the extraction centrifuges and the detection cells was fulfilled by a degasser (booster), which is also needed to overcome the backpressure from the detection cells. Flushing the solution with Ar is necessary to remove the dissolved air in the organic phase and scintillation mixture. Another advantage of the gas-wash step is to make calibration possible and convenient via the flushing gas. The ^{227}Ac-source supplying the short-lived ^{219}Rn gas (radionuclide generator) is applied for calibration during TAE experiments.

To be able to unambiguously confirm the detection of a TAE, a single detected α event is not sufficient for a positive identification of the desired TAE studied. Positive identification of a single TAE atom can often be made by detection of the time-correlated α-decays of the TAE parent and the resulting daughter. When an α emitter is observed in the selected energy window a valve closes the detector flow cell. The cell remains closed for a certain time or until the decay of the daughter is observed. The time between the two decays is registered and used in the off-line analysis after the experiment. The technique of α-α correlations in liquid-liquid scintillation is described in [16, 51, 107].

ii. Detector Cells

As indicated above, on-line α liquid scintillation measurement is performed in a detector cell through which the scintillator solution is continuously pumped. The shape, size and choice of materials in the detector cell impact the energy resolution, and the cell shape and size control the hold-up time (residence time distribution) of the solution in the cell. A detailed drawing of the detection cell is shown in Fig. 3.13. The flow cell is made in a 70 mm wide piece of Teflon with a meander-shaped flow track. A 1 mm thick disk of Kel-F and 80 mm long cylindrical light guide are mounted on top of the Teflon piece to conduct and spread the scintillation light evenly over the window of a 3- inch photo-multiplier tube. The volume of the cell is 5.5 ml. Several detection cells can be mounted in series enabling detection of radionuclides with longer half-lives than the hold-up time of a single detection cell.

As briefly mentioned above, α-particles from ^{219}Rn and ^{215}Po are employed to calibrate the detection cells, and a ^{227}Ac source (1.7 kBq on beryllium foil) is available for this purpose. The 3.96 s ^{219}Rn is a member of the ^{227}Ac decay chain. In the booster step He gas is

passed over the ^{227}Ac source, allowing ^{219}Rn to dissolve in the scintillation solution before entering the detector cells. ^{219}Rn emits α-particles of several energies, with the most pronounced at 6.819 MeV (79.4%), 6.553 MeV (12.9%) and 6.425 MeV (7.5%) [107]. The daughter product, ^{215}Po, decays with a half-life of 1.78 ms, by α-particle emission of 7.386 MeV (100%) [108].

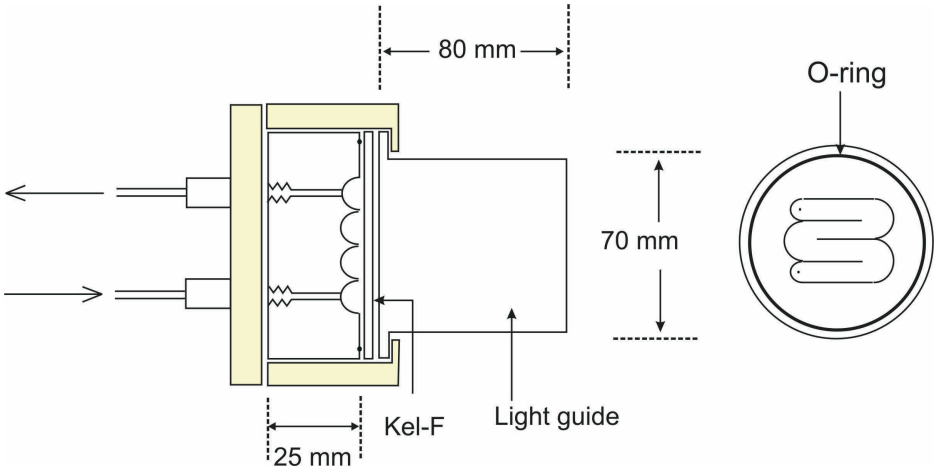

Fig. 3. 13 A schematic drawing of the meander cell, used for continuous liquid-scintillation detection of α particles

α Liquid-scintillation detection has relatively poor energy resolution compared to plate-counting solid-state detectors. However, with careful selection of the liquid-scintillation cocktail, energy resolution of about 300 keV full width at half maximum (FWHM) for 6.5~7.5 MeV α particles can be achieved [16].

4 Experimental Procedures

4.1 Procedure in Model Experiments

Both batch experiments and on-line SISAK experiments were conducted to develop suitable separation systems for a future Db SISAK study.

4.1.1 Batch Experiments and Measurement

The batch liquid extraction experiments were carried out with equal volumes (3 mL) of organic and aqueous phases in test tubes at room temperature (20–25ºC). The two phases were thoroughly mixed in a mechanical shaker for an equally long time, e.g., 2 minutes and 45 seconds. After phase separation, aliquots of each phase were withdrawn and the extraction distribution ratios were determined by measuring the activities in each phase by γ-ray spectroscopy using an HPGe detector.

Tracers and stock solution

For the batch experiments, carrier-free niobium tracer, ^{95}Nb ($T_{1/2}$ = 35 d), was obtained by irradiating 1 mg UO_3, enriched to 88% in ^{235}U, with thermal neutrons in a thermal neutron flux of $1.1 \cdot 10^{13}$ n/(cm^2·s) for 72 hours. ^{95}Zr ($T_{1/2}$ = 64 d) was isolated from the fission mixture. ^{95}Nb could then be obtained as a decay product from ^{95}Zr.

The non-carrier-free tantalum tracer, ^{182}Ta ($T_{1/2}$ = 114.4 d), was produced by irradiating 12.5 mg tantalum metal foil. The carrier-free protactinium tracer, ^{233}Pa ($T_{1/2}$ = 27 d), was obtained as a decay product from ^{233}Th ($T_{1/2}$ = 22.3 min) produced by irradiating 6 mg

$Th(NO_3)_4$ under the same irradiation conditions as described above. The reactor JEEP II at the Institute for Energy Technology (IFE) was used for all neutron irradiations.

The stock solution of tantalum was prepared by dissolving the tantalum metal foil in 1 mL concentrated HNO_3 with 20 drops of concentrated HF added during heating in a polyethylene vial. After evaporating to dryness, the residue was dissolved in 0.5 mL concentrated HNO_3 and again heated until dryness. Finally, the residue was dissolved in 4.5 mL 3.5 M H_2SO_4.

Preparation of stock solutions of ^{95}Nb was performed by dissolving the irradiated UO_3 in 0.5 M H_2SO_4. From this solution, carrier-free Zr was extracted with 0.05 M TOA in toluene (5 mL of each phase). The radionuclide ^{95}Zr, which produces niobium tracer, was stored in the organic solution.

Carrier-free protactinium stock solutions were prepared by directly dissolving the irradiated $Th(NO)_3$ in 1 ml water.

Experimental errors

In the extraction experiments the overall experimental error is caused mainly from two sources:

- the uncertainty in measuring the amount of radioactivity
- the uncertainty in withdrawing samples from each phase, due to pipetting errors and entrainment of the wrong phase.

The contribution of the former to the total experimental error was less than 2~3% in most experiments. The direct pipetting error (i.e. volume error) is less than 2%. The error due to entrainment of the wrong phase is highly dependent on the distribution value: For very low or very high distribution values small amount of the wrong phase can significantly increase the measured activity in the phase which should have nearly no activity. The experiments were performed with at least four parallels for each point of the extraction curves. The presented distribution ratios are the mean values of the parallel measurements and the error bars based on the variation between the parallels.

4.1.2 SISAK on-line Experiments

The schematic setup of the SISAK Db model experiments is illustrated in Fig. 4.1. Compared to the general SISAK setup for performing transactinide experiments in Fig. 3.9, it is clear that the setup for model experiments is much simpler. This is because the model experiments use γ measurements to determine the amount of activity in each phase, which is much simpler to do than the on-line liquid scintillation detection used in the transactinide experiments. However, it should be emphasised that all the parts up to and including the main extraction stage is identical. Thus, the setup for model experiments provides exactly the same experimental conditions as those of a transactinide experiment.

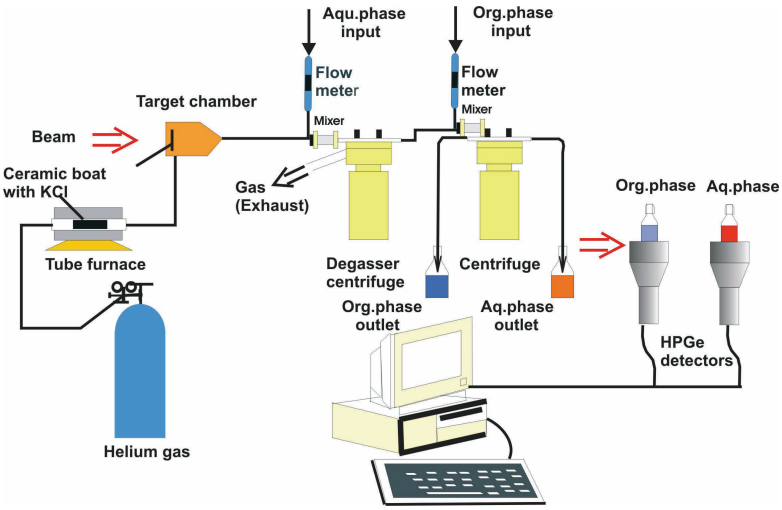

Fig. 4. 1 Schematic setup of the SISAK Db model experiments.

Carrier-free tantalum and niobium tracers were produced by ^{3}He irradiation of suitable targets (for details, see below). During ^{3}He irradiation, the produced radionuclides recoil out from the backside of the target and are stopped in the sweeping helium gas. The He gas contains KCl-aerosol clusters, to which the ions recoiling out of the target will be attached, and thus swept out of the target chamber continuously. The gas-jet flow rate was 0.5 L/min. The reaction products are then transported through a capillary to the SISAK separation system. Here, they are dissolved in an aqueous phase heated to about 80˚C. The dissolution takes place in a gas/liquid mixer. Possible gaseous reaction products and the He carrier gas

are then removed in a degasser unit. After degassing the aqueous phase is contacted with an organic solution containing the extracting agent trioctyl amine (TOA) or Aliquat 336 through a liquid/liquid mixer and the mixed phases are fed into the centrifuge and separated. Flow rates were typically 0.40 mL/s for both phases. After phase separation the organic and aqueous phases are simultaneously collected and measured on γ-ray HPGe detectors. Sample collecting and counting times depend on the half-lives of the radionuclides in question.

Tracers and Chemicals

In the SISAK experiments, carrier-free tantalum tracer, ^{178}Ta ($T_{½}$ =2.45 h) and carrier-free niobium tracers, ^{88}Nb ($T_{½}$= 14.3 min) and ^{88m}Nb ($T_{½}$= 7.8 min), were obtained by irradiation of a target of natural hafnium and a target of natural yttrium, respectively, with a 45-MeV ^{3}He-particle beam. The beam energy reduces to approximately 42 MeV at the target. The beam intensities for producing the Nb- and Ta- tracers are around 300 enA and 600 enA, respectively. All irradiations were carried out at OCL. For production of ^{178}Ta ($T_{1/2}$ = 2.45 h), the nuclear reaction is ^{178}Hf (^{3}He,p2n)^{178}Ta. For ^{88m}Nb ($T_{1/2}$ = 7.8 min) and ^{88}Nb ($T_{½}$ = 14.3 min), the nuclear reactions are ^{89}Y (^{3}He, 4n) ^{88m}Nb and ^{89}Y (^{3}He, 4n) ^{88}Nb.

TOA, a tertiary amine with three octyl groups attached to a nitrogen atom (see Fig. 4.2), was obtained from Merck Schuchardt OHG 85662 Hohenbrunn, Germany. Some physical properties of TOA are presented in Table 4.1.

Table 4.1 Some physical properties of TOA

Property	
Formula	$(CH_3(CH_2)_7)_3N$
Molar mass	353.68 g/mol
Density	0.81 kg/L
Purity	93%

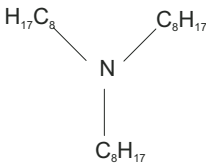

Fig. 4. 2 Structure of TOA

Aliquat 336, quaternary ammonium salt with one methyl group and three longer alkyl chains (C8–C10) attached to nitrogen, yielding a positive charge at the nitrogen atom (see Fig. 4.1), were obtained from Sigma Aldrich.Therefore, a chloride ion is attached to the nitrogen atom. Some physical properties of Aliquat 336 are shown in Table 4.2.

Table 4. 2 Some physical properties of Aliquat 336

Property	
Formula	$CH_3N[(CH_2)_7CH_3]_3Cl$
Molar mass	404.17 g/mol
Density	0.88 g/cm^3

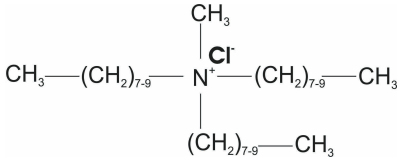

Fig. 4. 3 Structure of Aliquat 336

Table 4. 3 Some physical properties of H_2O_2, H_2SO_4 and toluene

Property	Hydrogen peroxide	Sulphuric acid	Toluene
Formula	H_2O_2	H_2SO_4	
Molar mass	34.01 g/mol	98.08 g/mol	92.14 g/mol
Density	1.13 g/cm^3	1.84 kg/L	0.8669 g/cm³

Hydrogen peroxide (about 35%) was provided by VBR Internatioal AS. Sulphuric acid and toluene with claimed purities of 95–97% and 100%, respectively, and potassium sulphate p.a. were provided by Merck KGaA, Darmstadt, Germany. Hydrofluoric acid (40%) was obtained from Fluka. All acid solutions are made with deionised water.

Experimental Error

The experimental error for the on-line experiments is a function of several factors, e.g. the concentrations of the aqueous and organic solutions, the flow rates in each of the two phases, the uncertainty in the radioactivity measurement, the phase purity of the two phases out of the centrifuge, etc. The contribution to the overall error from these sources can be kept low by carefully using standard laboratory practices during the experiments. However, even in carefully carried out experiments, the entrainment of small droplets of one of the phase in the other might distort the results, especially for very low or high distribution ratios. On-line monitoring by optical phase purity meters, and visual inspection of the samples ensured that the errors due to entrainment were kept to a minimum. The presented distribution ratios are mean values of several parallel measurements.

4.2 Procedure in TAE Experiments

The Berkeley Gas-filled Separator (BGS) coupled to the 88-inch cyclotron at Lawrence Berkeley National Laboratory (LBNL) was used for preseparation of the EVRs from the

^{208}Pb(^{50}Ti,n)^{257}Rf reaction and the ^{257}Rf-ions were selected and focused to enter the RTC, then became attached to the KCl aerosols carried by helium gas and were sucked through a 20 m tube to the SISAK chemical separation system. The BGS and the RTC are explained in more detail in chapter 3.2 and Paper IV.

It should be noted that the SISAK experiments were performed with the 4.7 s Rf isotope instead of with the much longer lived 78-s ^{261}Rf. The later is commonly used in the chemistry experiments using other techniques. The reason is that the relatively asymmetric "hot fusion" reactions used for producing 78-s ^{261}Rf transfer little kinetic energy (about 6.8 MeV for the ^{248}Cm(^{18}O, 5n)^{261}Rf reaction and about 9.5 MeV for ^{244}Pu(^{22}Ne,5n)^{261}Rf) to the Rf ions recoiling out of the target. This is not enough to penetrate the window between the separator chamber and the RTC. Hence, the more symmetric "cold fusion" reactions for producing ^{257}Rf, which transfer enough energy (45.5 MeV for ^{208}Pb(^{50}Ti,n)^{257}Rf) to push the recoils through the 6 μm mylar window, must be used. The window between the separator and the RTC is necessary due to substantial pressure difference: The separator is typically operated at around 1 mbar and the gas-jet transfer line connected to the RTC is operated at 1.4–1.8 bars for SISAK experiments.

The focusing and production rates of the ^{257}Rf ions are checked by inserting a silicon-strip detector in front of the RTC window. In addition, the production rate is continuously monitored by measuring the amount of ions Rutherford scattering from the target onto two pin detectors positioned $\pm 27^{o}$ incident to the beam.

During the experiments in 2003, Setup B (see Fig. 3.3) was used to measure the amount of Rf extracted from 0.5 M H_2SO_4 solution into 0.02 M TOA in toluene. This TOA concentration was selected to ensure that Rf would be extracted, which is important since only the organic phase can be measured. Both Zr and Hf extract with high yield at this TOA concentration. In Setup B, the liquid/liquid mixers were used in front of the centrifuges. They consisted of a tube with a length of 43 mm and an internal diameter of 8 mm. The tube was stuffed with PEEK wool (Fig. 3.4, Mixer C). In front of the last degasser, usually referred to as the booster because it helps pump the scintillator solution through the detector cells, there is another mixer, a traditional SISAK "Zigzag" type (see Fig. 3.4, Mixer B) with a length of 45 mm. This mixer serves two purposes: 1) Thorough mixing of the organic

phase and scintillator and 2) Flushing the scintillator cocktail with He to remove O_2, due to the quenching effect it has on the scintillation process.

Two detector cells were used for measuring ^{257}Rf-^{253}No α-α correlation in this experiment. In addition, one detector cell was used to monitor the scintillation performance using a ^{137}Cs source to generate Compton electrons in the liquid as described in [107].

For calibration a ^{227}Ac source was used. As mentioned previously, it emanates ^{219}Rn which is carried with the He (two 3-way valves are used to either include or bypass the source). ^{219}Rn disintegration is quickly followed by disintegration of ^{215}Po, which gives two αs in quick succession. The α pairs can be identified in the Data Stream and used to calibrate the detectors. For each of the two main detectors, the number of counts in the Rutherford scattering detectors was measured when the cell was open.

During the experiments in 2005 a more advanced setup was used, which enabled simultaneous measurement of the activity in both phases (Fig. 3.3 setup C). The advantage of the advanced setup is that uncertainty in the gas-jet performance is eliminated. In the simple setup only activity in the organic phase can be measured. In Setup C, the 1/4″ PFA tubes normally used to connect the various units was substituted by 1/8″ tubes if the connection transported activity. This decreases transport time through the system. Another modification done to decrease the transport time was to reduce the size of the valve heads: All throttles (for phase separation adjustments) which were not strictly needed were removed. Another new addition was the ability to quickly and simply measure the residence time through any part of the system by using coloured solutions. This is much quicker and easier than using pulsed beams or purposely injected radiotracers and was used to accurately measure the delay caused by the second extraction step. This delay must be known in order to correct for the decay loss caused by the second centrifuge when distribution values are to be calculated [17, 109]. The delay for a total flow of 0.84 ml/s, as used in the second experiment, was calculated to be 4.1 s. This value was then used to calculate the delay loss due to the second extraction step.

There are two ways to use this setup to measure the distribution ratio of the first extraction stage. One is to use an extractant in the second stage which has nearly 100% extraction efficiency. The distribution ratio, *D*, will then be given by

$$D = \frac{R_{org1}}{R_{aq1}} = \frac{R_{org1}}{f \bullet R_{org2}} \qquad \text{Eqn. 5.1}$$

where R denotes the activity in the phases indicated by the subscripts. The factor *f* is used to correct the R_{org2} value if the extraction is not 100% in the second stage. A problem with this method is that the factor *f* might not be very well known. In that case, an alternative is to use the same extractant in the first and second stages, i.e., both stages will have the same distribution ratio. The distribution ratio can then be calculated from the measured activity in the two organic phases according to:

$$D = \frac{R_{org1} - R_{org2}}{R_{org2}} \qquad \text{Eqn. 5.2}$$

For this experiment a TOA concentration was selected such that if Rf behaved as Zr, it would extract and if it behaved more like Hf it would not extract.

5 Results and Discussion

5.1 Studies on Extraction of Nb, Ta and Pa from H_2SO_4

The requirements of a SISAK liquid-liquid extraction system suitable for transactinide experiments in general and dubnium in particular, due to short half-lives and low production rates, are:

i) the extraction system needs to achieve sufficient separation from all interfering radionuclides;

ii) the system needs to have suitable distribution ratios for experiments with very few events. This implies that the distribution ratio must be kept between 0.1 and 10 to be able to observe events in both phases;

iii) the extraction involved needs to have fast reaction kinetics to allow the transactinide to be detected;

iv) the system should have good phase separation and the chemicals involved should be easy to handle;

v) the system should be selective between the lighter homologues of the element of interest.

vi) the reagents must not quench or interfere with the liquid scintillation process used for α detection.

5.1.1 Distribution Ratio of Nb, Ta and Pa in H_2SO_4/TOA system

The TOA/H_2SO_4 chemical system was successfully applied in 2003 in Rf SISAK experiments at LBNL (see Paper IV). The difference in TOA extraction of Zr and Hf from H_2SO_4 solutions is large enough to make SISAK experiments feasible for distinguishing between Zr- or Hf-like behaviour of element 104. From the extraction sequence, chemical properties such as the stability of the extracted complexes can be determined [109]. Based on the positive experience gained from these experiments, there was incentive to investigate whether the same extraction system could be applied to Ta and Nb. Experiments to investigate if the TOA/H_2SO_4 system could also be used for studying Db were then carried out at OCL. The Group-5 elements Nb and Ta were used in these investigations, which were carried out both as batch experiments and as on-line experiments using the SISAK system. In addition, in batch experiments the Group-5 pseudo-homologue Pa was also investigated. The results of these experiments are reported in Paper I. Below is a summary of the results.

Fig. 5.1. shows the dependence of the distribution ratios of Ta, Nb and Pa on H_2SO_4 concentration in the batch experiments. The distribution ratios increase at low acidities and reach a maximum at around 0.10 M H_2SO_4 and decrease at higher acidities. The increase towards a maximum might be ascribed to the salting-out effect caused by the sulphuric acid. The decrease at higher acidity might be explained either by competition for the TOA extractant between the metal species (Ta, Nb and Pa) and the sulphuric acid or by the formation of less readily extractable complexes [110, 111]. In the batch experiment it is interesting to note that Ta behaves more like Pa than Nb.

Under the same range of H_2SO_4 and TOA concentrations, we further conducted SISAK experiments. Due to poor phase separation at low acidities, the effect of increase in the ionic strength was tested by addition of K_2SO_4 to the aqueous phase in concentrations of 0.25 M K_2SO_4 and 0.15 M K_2SO_4, respectively. The result is shown in Fig. 5.2 and Table 5.1. At low acidities, distribution ratios of both Ta and Nb are clearly higher in 0.15 M K_2SO_4 than in 0.25 M K_2SO_4, while with the increase of acidity such a difference becomes insignificant. This might be explained by the fact that the difference of concentrations of the ligands, HSO_4^- or SO_4^{2-}, in solutions decreases with increasing H_2SO_4 concentration as illustrated in

Fig. 5.12. At low acid concentration, the difference of H^+, $HSO4^-$ and SO_4^{2-} concentrations in solutions with 0.15 M K_2SO_4 and 0.25 M K_2SO_4 is significant. At high acid concentration such difference becomes insignificant. The D-values of Ta and Nb decreased relative to the batch experiments while the phase separation improved. The lower D-values in the on-line experiments may possibly be explained by increased competition for the available TOA by the increased concentration of SO_4^{2-}/HSO_4^- [24] (see Fig. 5.12). Possible different valence states of the nuclides in the batch and on-line experiments are another factor which may affect the D-value. However, the general trends of Nb and Ta D-value curves are the same as those from the batch experiments. From 0.020 M to 2.0 M H_2SO_4 the separation factors for Nb/Ta range from 2.9 to 9.2 for 0.15 M K_2SO_4 and from 2.1 to 13.1 for 0.25 M K_2SO_4. D values of Ta are between 0.16 and 1.78 for 0.15 M K_2SO_4 and between 0.05 and 1.61 for 0.25 M K_2SO_4. D values of Nb are between 0.47 and 9.54 in 0.15 M K_2SO_4 and between 0.11 and 11.4, see Table 5.1. With 0.25 M K_2SO_4 present in aqueous solution the extraction of Nb and Ta with 0.20 M TOA in toluene was also investigated as illustrated in Fig. 5.3. It shows that 0.20 M TOA gives expectedly higher values of distribution ratios of both Nb and Ta and the separation factors range from 2.1 to 15.5. D values of Nb and Ta are 0.32～19.32 and 0.15 ～2.6, see Tab. 5. 3. 2**.**

5.1.2 Effect of TOA on the Distribution Ratio of Nb, Ta and Pa

A series of batch extractions were performed to measure D-values for Ta, Nb and Pa (in 0.25 M sulphuric acid) as a function of various TOA concentrations at 0.25 M H_2SO_4, shown in Fig. 5.4. In general, the D-values increase with increasing concentration of TOA, Nb is extracted with higher yields than Ta and they are well separated. As before, Pa is extracted with higher yield than Ta, but they follow the same trend. Again, one observes that the behaviour of Pa is more similar to Ta than to Nb and reflects the ionic similarity of the species of Ta and Pa and the ionic variety of Nb. This is in agreement with the result in Fig. 5.1. The slopes of Nb, Ta and Pa extraction curves are found to be 0.36±0.03, 1.3±0.1 and 1.3±0.1, respectively.

Based on the result obtained from the batch experiment, the SISAK on-line experiment was also performed with 0.10 M, 0.25 M and 0.50 M H_2SO_4 respectively. D-values for extraction of Ta, Nb as a function of various TOA concentrations at 0.10 M, 0.25 M and

0.50 M H_2SO_4 are illustrated in Fig. 5.5. The results show that D-values of Nb and Ta are the highest at 0.25 M H_2SO_4 and the lowest at 0.10 M H_2SO_4. The separation factors and D-values are shown in Table 5.3. The slopes of Nb extraction curves from the SISAK experiments are found to be 0.39±0.01, 0.58±0.05 and 0.46±0.04 for 0.10 M, 0.50 M and 0.25 M H_2SO_4, respectively, and the corresponding slopes of Ta extraction curves are 0.90±0.01, 0.87±0.1 and 1.11±0.02, (see Fig). With respect to the extraction curve for 0.25 M H_2SO_4, the measurements in high TOA concentration deviated from the linear trend observed for batch experiments (Fig. 5.4); thus, the D-values for 0.20 M TOA (the highest value) were not included in the determination of the fitted slope of the extraction curve.

The γ-ray spectra obtained from organic phase in the extraction of Ta and Nb from 0.50 M H_2SO_4 into 0.20 M TOA/toluene are shown in Fig. 5.6.

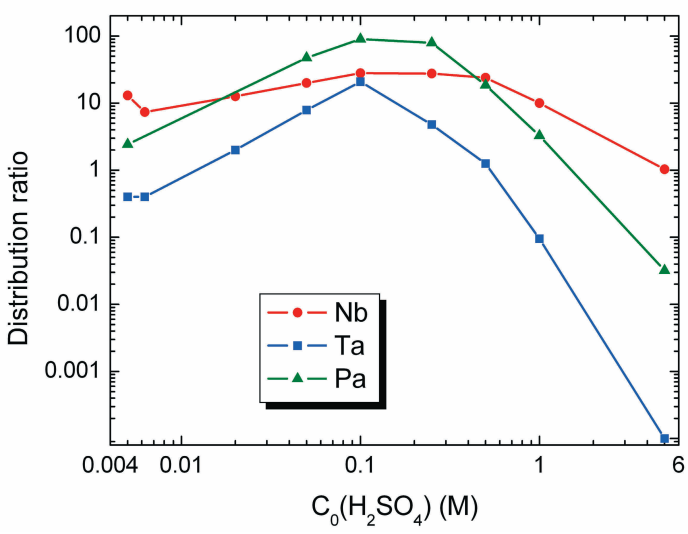

Fig. 5. 1 Results from batch extraction of tantalum, niobium and protactinium from various initial (C_0) H_2SO_4 concentrations. The metal complexes were extracted into solutions of 0.10 M TOA in toluene.

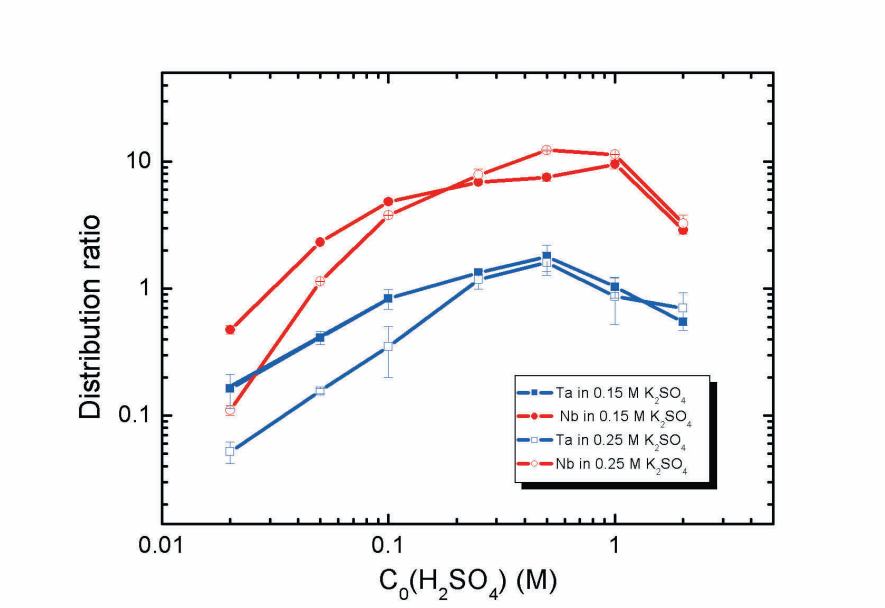

Fig. 5. 2 Results from SISAK on-line extraction of tantalum and niobium from 0.15 M and 0.25 M K_2SO_4 solutions with various initial (C_0) H_2SO_4 concentrations. The metal complexes were extracted into solutions of 0.10 M TOA in toluene.

Table 5. 1 Distribution ratios and separation factors for Nb/Ta (SF) with 0.15 M K_2SO_4 or 0.25 M K_2SO_4 in various H_2SO_4 concentrations and 0.10 M TOA in toluene

H_2SO_4 (M)	0.15 M K_2SO_4			0.25 M K_2SO_4		
	D (Ta)	D (Nb)	SF	D (Ta)	D (Nb)	SF
0.02	0.16	0.47	2.9	0.05	0.11	2.2
0.05	0. 40	2.32	5.8	0.15	1.14	7.6
0.1	0.83	4.84	5.8	0.35	3.79	10.8
0.25	1.34	6.89	5.2	1.18	7.87	6.7
0.5	1.78	7.53	4.2	1.61	12.3	7.6
1	1.04	9.54	9.2	0.87	11.4	13.1
2	0.55	2.89	5.3	0.7	3.24	4.6

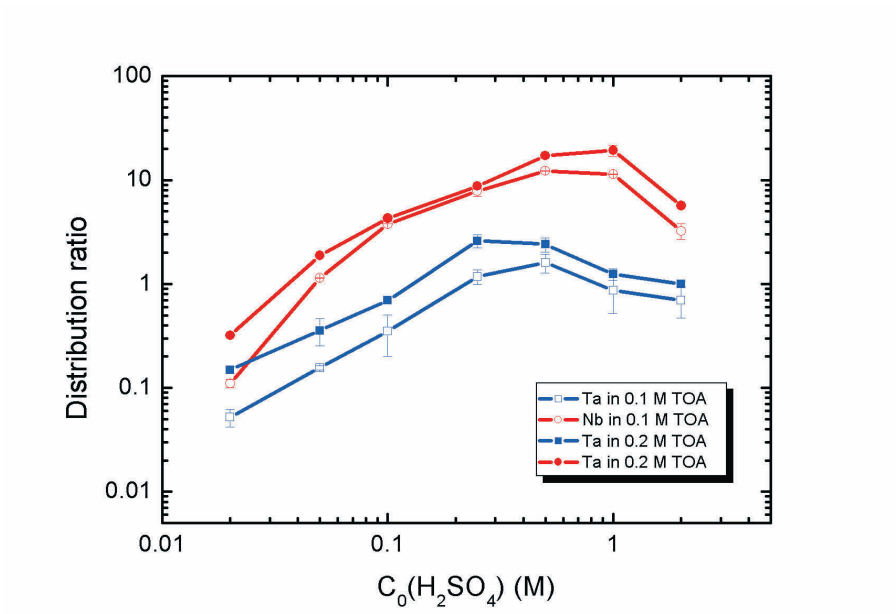

Fig. 5. 3 Results from SISAK on-line extraction of tantalum and niobium from 0.25 M K_2SO_4 solutions with various initial (C_0) H_2SO_4 concentrations. The metal complexes were extracted into a solution of 0.10 M and 0.20 M TOA in toluene

Table 5. 2 Distribution ratios and separation factors for Nb/Ta (SF) with 0.10 M and 0.20 M TOA from various initial H2SO4 concentrations with 0.25 M K2SO4

H_2SO_4 (M)	0.10 M TOA			0.20 M TOA		
	D (Ta)	D (Nb)	SF	D (Ta)	D (Nb)	SF
0.02	0.05	0.11	2.2	0.15	0.32	2.1
0.05	0.15	1.14	7.6	0.36	1.88	5.2
0.1	0.35	3.79	10.8	0.70	4.29	6.1
0.25	1.18	7.87	6.7	2.6	8.75	3.4
0.5	1.61	12.3	7.6	2.4	17.16	7.1
1	0.87	11.4	13.1	1.24	19.32	15.5
2	0.7	3.24	4.6	1.0	5.66	5.7

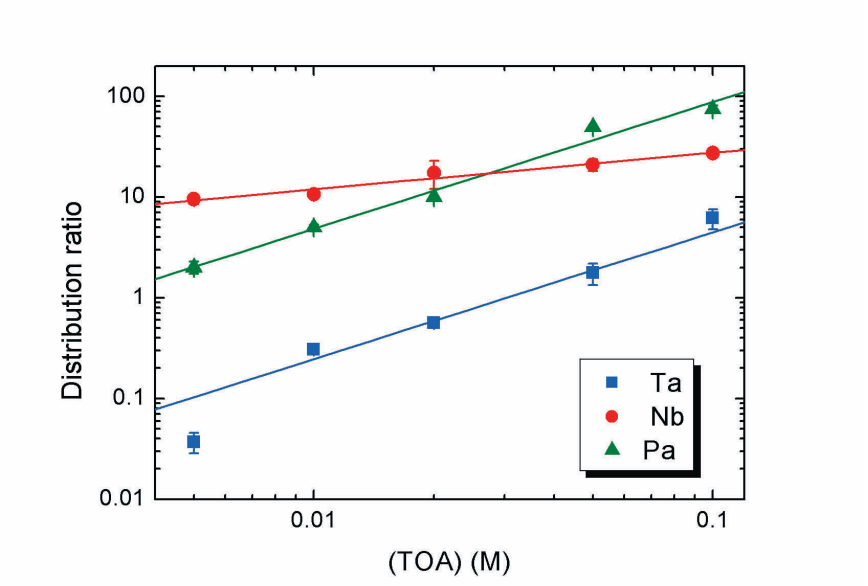

Fig. 5. 4 Batch extraction of tantalum, niobium and protactinium from 0.25 M H_2SO_4 with various concentrations of TOA in toluene

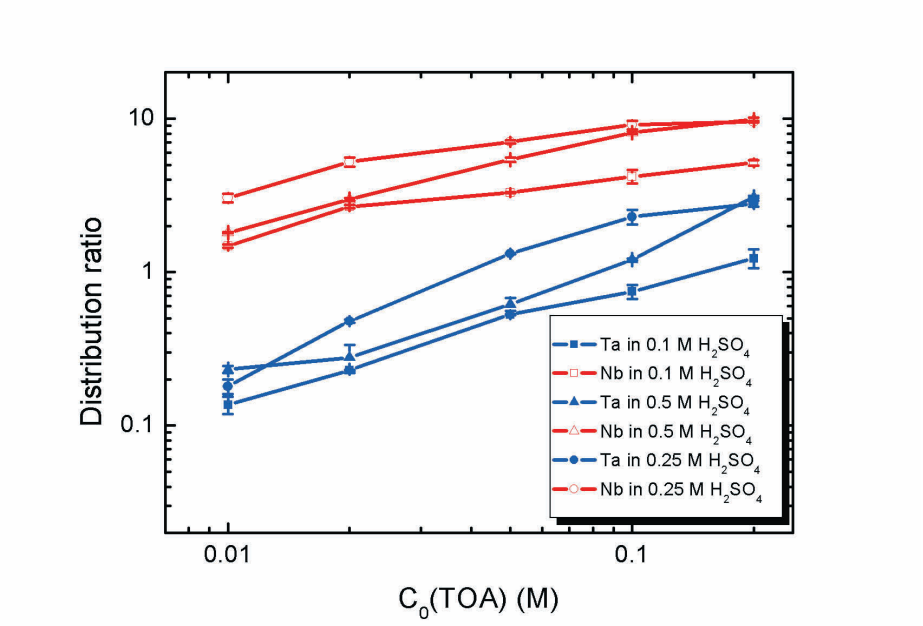

Fig. 5. 5 SISAK on-line extraction of tantalum and niobium from 0.10 M, 0.25 M and 0.5 M H_2SO_4, respectively, with various concentrations of TOA in toluene

Table 5. 3 Distribution ratios and separation factors for Nb/Ta (SF) with 0.10 M TOA in toluene from 0.10 M, 0.25 M and 0.50 M H_2SO_4 solutions

TOA (M)	0.10 M H_2SO_4			0.50 M H_2SO_4			0.25 M H_2SO_4		
	D(Ta)	D(Nb)	SF	D(Ta)	D(Nb)	SF	D(Ta)	D(Nb)	SF
0.01	0.14	1.48	10.6	0.23	1.81	7.9	0.18	3	16.7
0.02	0.23	2.67	11.6	0.28	2.98	10.6	0.48	5.2	10.8
0.05	0.53	3.29	6.2	0.62	5.4	8.7	1.32	7.1	5.4
0.1	0.75	4.2	5.6	1.2	8.1	6.7	2.29	9.1	4
0.2	1.23	5.16	4.2	3.1	9.84	3.2	2.79	9.5	3.4

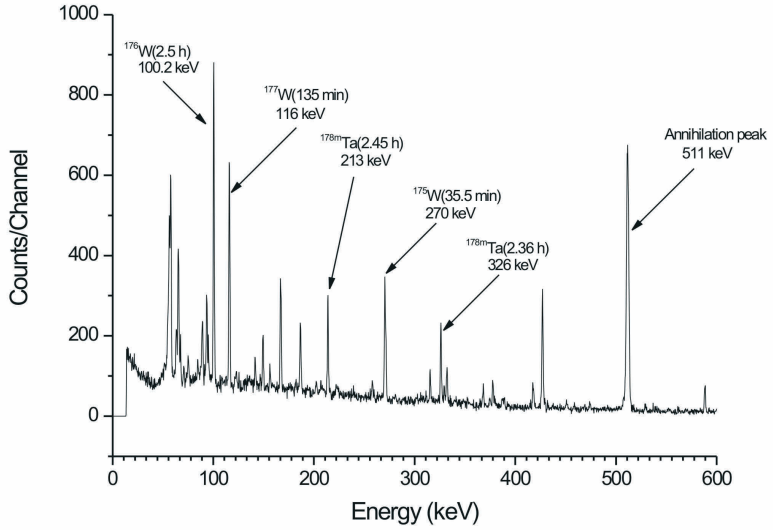

(a)

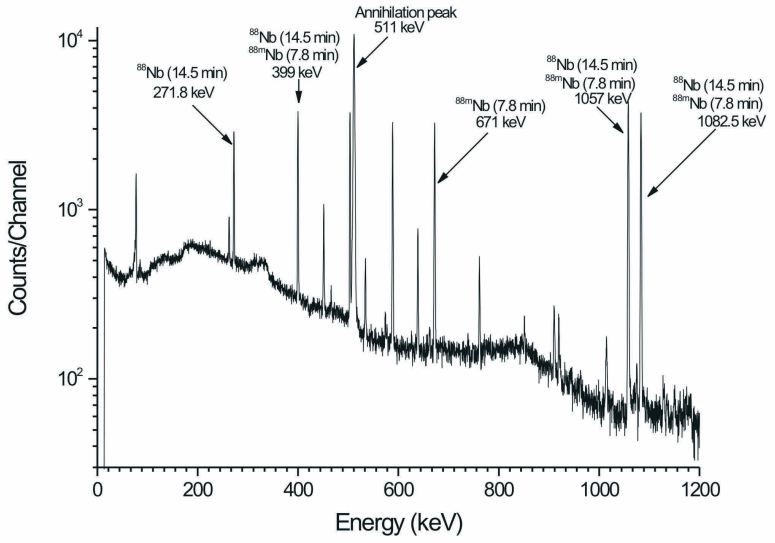

(b)

Fig. 5. 6 γ-ray spectra obtained from organic phase in the extraction of Ta from (a) 0.5 M H_2SO_4 into 0.2 M TOA/toluene in the reaction $^{3}He + ^{nat}Hf$ used for production of ^{178}Ta (T ½ =2.45 h) and (b) the extraction of Nb from 0.5 M H_2SO_4 into 0.2 M TOA/toluene in the reaction $^{3}He + ^{nat89}Y$ used for production of ^{88}Nb (T ½ =14.5 min) and ^{88m}Nb (T ½ =7.8 min). Acquisition of the spectra was started after a 7-min sampling and a 1-min gap. Measuring time was 9 min. γ-lines of different radionuclides of Nb, Ta and W were observed and labelled.

5.1.3 Extraction Kinetics of Pa, Nb and Ta in the H_2SO_4 /TOA System

The extraction kinetics of Nb and Ta were investigated in both batch and SISAK on-line experiments. For batch experiments the mixing time is the shaking time of the test tubes (by a mechanical shaker). Fig. 5.7. shows the distibution ratio of Pa as a function of shaking time in 0.5 M H_2SO_4/0.1 M TOA solutions; it takes about 100 seconds for Pa to reach equilibrium. Similar kinetics experiments with Nb and Ta were also performed: It takes about 15 seconds for Nb to reach extraction equilibrium at 0.1 M TOA/1 M H_2SO_4, see Fig. 5.8. It takes around 200 s for Ta to reach extraction equilibrium at 0.1 M TOA/0.25 M H_2SO_4 solutions, shown in Fig. 5.9.

With the SISAK equipment the investigation on extraction kinetics of Nb and Ta is realized by applying different lengths of the static mixer to measure the effect of the contact time on the extraction efficiency while the other parameters were kept constant.

Mixer lengths varied from 29 mm to 130 mm (see Fig. 5.10). The measured mean liquid hold-up time for the 44 mm mixer with the applied volumetric flow rate of 0.4 mL/s is 0.5 s. Fig. 5.10 shows that extraction equilibrium for both Nb and Ta has been reached already with the shortest mixer of 29 mm. This implies that extraction equilibrium time is < 0.5 s (even < 0.33 s provided equal porosity and packing conditions for the mixers at 29 mm and 44 mm). This is acceptable for efficient SISAK experiments. Obviously, the extraction kinetics in the SISAK experiments is much faster than in the batch experiment. This may be explained by the following consideration:

The metal ions of Nb and Ta are supposed to be highly hydrolyzed in the batch experiments while the freshly produced ions in the SISAK experiments are expected to be less hydrolyzed. Considering the probable extraction mechanism, one may expect that time to extraction equilibrium is slower for the hydrolyzed species than for the anionic sulphate- or bisulphate-complexed species.

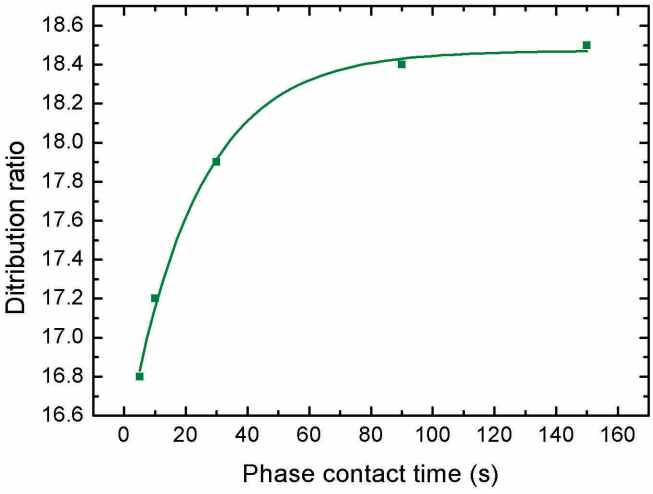

Fig. 5. 7 Distribution ratio of Pa as a function of phase contact time in an extraction system composed of 0.5 M H_2SO_4 into 0.1 M TOA in toluene with batch experiments.

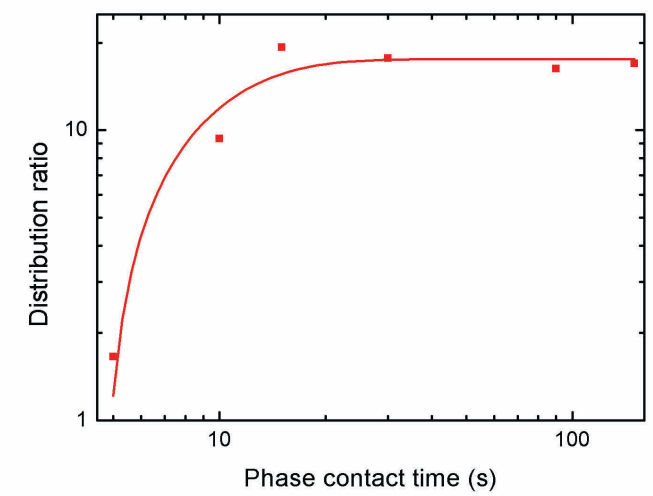

Fig. 5. 8 Batch extraction experiments of Nb from 1.0 M H_2SO_4 into 0.10 M TOA in toluene as a function of phase contact time.

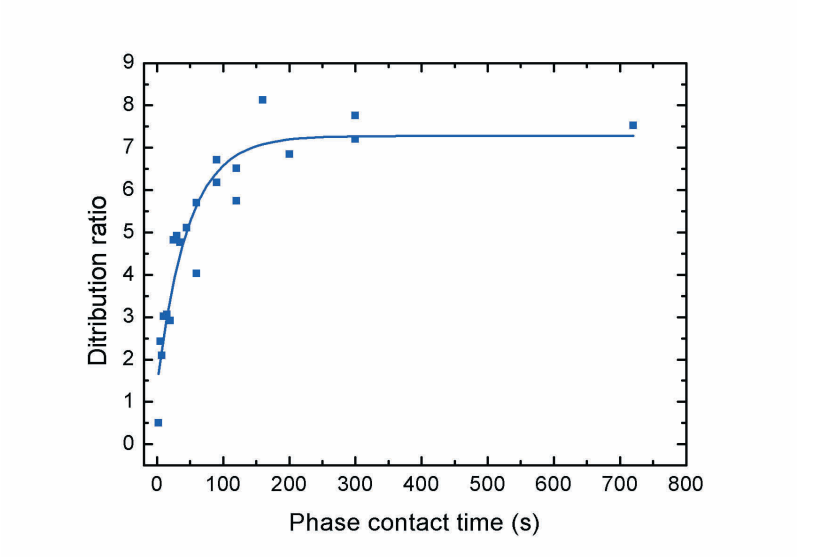

Fig. 5. 9 Batch extraction experiments of Ta from 0.25 M H_2SO_4 into 0.1 M TOA in toluene as a function of phase contact time.

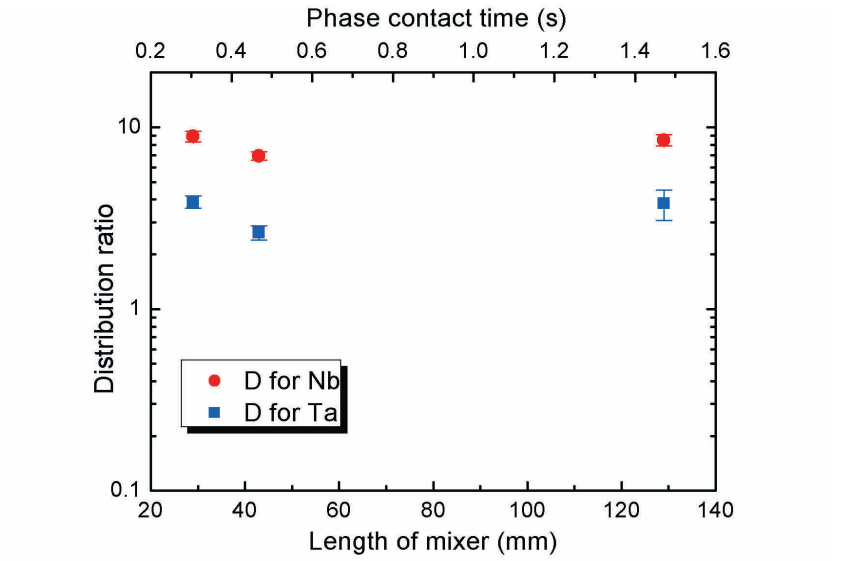

Fig. 5. 10 SISAK on-line extraction experiments of Ta and Nb from 0.25 M H_2SO_4 into 0.1 M TOA in toluene at a volumetric flow rate of 0.40 mL/s for both phases as a function of the length of the static PEEK wool mixer.

5.1.4 The Cluster Dissolution Efficiency

The cluster dissolution efficiency is evaluated by the ratio of the activity collected from the degasser aqueous outlet to the activity captured in the direct catch. As discussed in 5.3 for SISAK transactinide experiments, it is important to know the cluster dissolution efficiency in order to calculate the expected number of correlation events in detectors, since correction must be done for decay loss of short-lived TAE nuclides studied.

The experimental procedure is as follows:

1. In the first experiment the nuclear reaction products transported by the gas-jet are caught on a glass microfibre filter (Whatman, Grade “GF/C”) in a setup usually refereed to as a "direct catch" setup. Then the nuclides of interest caught by the filter are dissolved in H_2SO_4 solution and are measured for activity with an HPGe detector. The amount of sulphuric acid solution used is selected to match the amount sampled in step 2, see below.
2. In the second experiment the nuclear reaction products transported by the gas-jet are dissolved in a heated H_2SO_4 solution at about 80˚C through a gas/liquid mixer. Possible gaseous reaction products and the He carrier-gas are removed in a degasser unit. After degassing, the liquid exiting from the degasser is measured in the same HPGe detector for the amount of activity of interest.

The experimental results show that the efficiency varies with H_2SO_4 concentrations and ranges from 63% to 87%. The highest efficiency is measured at 0.1 M H_2SO_4 with the least viscosity, which is found to be 86% for Ta and 87% for Nb. At 2 M H_2SO_4 with the highest viscosity, the efficiency was found to be at the lowest values, namely 63% for Ta and 64% for Nb, respectively; see Fig. 5.11. and Table 5.4. The different viscosities of H_2SO_4 solutions might be one of the main reasons for the different efficiencies observed. For the relative viscosity of the H_2SO_4 solution, [112] is referred to. In the literature [15], similar investigation was performed with both HCl and Lactic acid using ^{28}Al activity and the efficiency values range between 50% and 100%. This efficiency also depends on the type of mixer, aqueous flow rate used and the ratio of mixer gas to liquid volume.

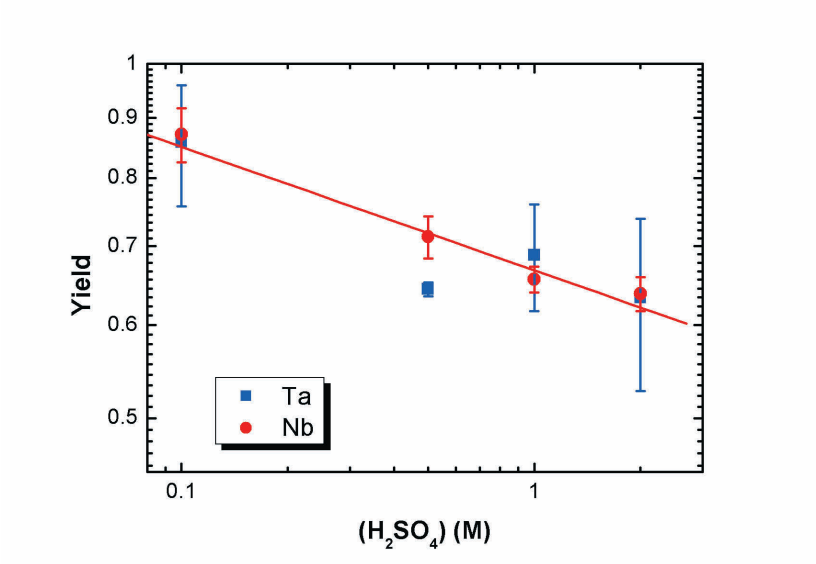

Fig. 5. 11 Cluster dissolution efficiency for Ta and Nb as a function of H_2SO_4 concentration

Table 5. 4 The efficiency of the cluster dissolution

Concentration of H_2SO_4	Relative viscosity	Efficiency for Ta	Efficiency for Nb
0.10 M	1.017	86%	87%
0.50 M	1.105	64%	71%
1.0 M	1.210	69%	66%
2.0 M	1.450	63%	64%

5.1.5 Dependence of the Concentration of H^+, HSO_4^- and SO_4^{2-} on H_2SO_4 Concentration

It is important to acquire knowledge about the concentration of all ligands present in the aqueous phase in order to analyze the possible extraction reactions and species formed in the extraction system. The calculation of concentrations of H^+, HSO_4^- and SO_4^{2-} in H_2SO_4 solutions with or without K_2SO_4 and $KHSO_4$ present was performed. As illustrated in Fig. 5.12, the results show that the concentrations of H^+ and HSO_4^- increase with the increase of H_2SO_4 concentration. The concentration of SO_4^{2-} decreases with the increase of H_2SO_4

concentration in solutions with K_2SO_4 or $KHSO_4$ present, and gradually increases in solution of H_2SO_4 without K_2SO_4 or $KHSO_4$ present. The amount of H^+ in solutions follows the sequence: 0.15 M $KHSO_4$>H_2SO_4>0.15 M K_2SO_4>0.25 M K_2SO_4; for SO_4^{2-} in solutions, the sequence is found to be 0.25 M K_2SO_4>0.15 M K_2SO_4>0.15 M $KHSO_4$>H_2SO_4; for HSO_4^-, the sequence is 0.15 M $KHSO_4$>0.25 M K_2SO_4≥0.15 M K_2SO_4>H_2SO_4. The details of these calculation are described in Appendix A5.

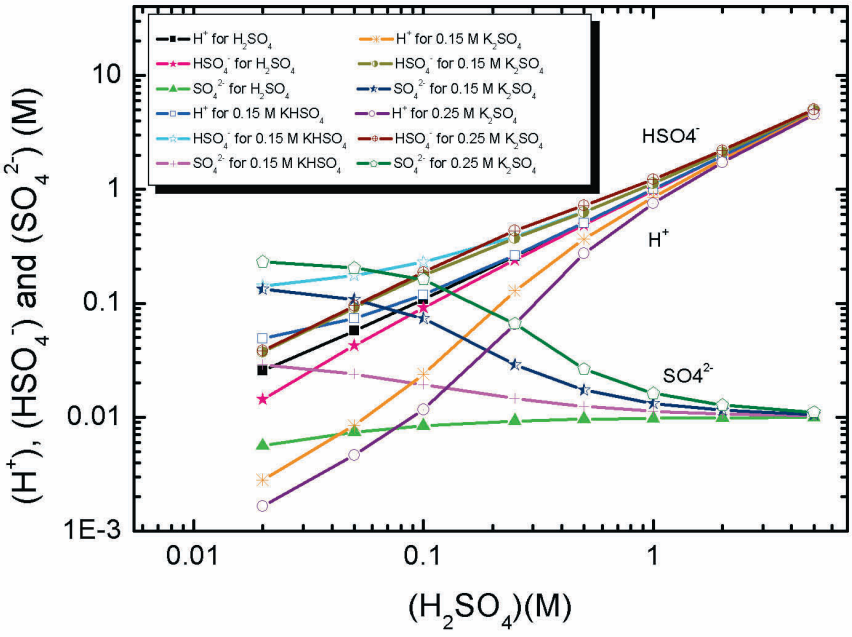

Fig. 5. 12 The concentration of H^+, HSO_4^- and SO_4^{2-} as a function of H_2SO_4 concentration with or without K_2SO_4 and $KHSO_4$ present

5.1.6 The Extraction of Ta and Nb in the H_2SO_4/TOA System with HF Present

Literature [113] shows that the sequence of the extraction of Nb and Ta by TOA in cyclohexane in the H_2SO_4 solution is Ta>Nb, which is different from what we have measured in the H_2SO_4/TOA system. The difference is suprising, as one would not expect that cyclohexane and toluene as solvents for this extraction system should behave rather different. The reason might be that the tracer solutions are essentially different in the two

experiments. The reference does not give details about the preparation of the tracer solutions for the cyclohexane experiments. However, according to an earlier work from the same institute, the Nb tracer is ^{95}Nb in hydrochloric acid medium and the Ta tracer is made of neutron activated metal powder which is subsequently dissolved in $HF+HNO_3$. After evaporation, the sample is dissolved in dilute HCl. The sequence of Ta and Nb extraction might be due to a small amount of HF still present in the solution. We performed some experiments to check the influence of HF in the H_2SO_4/TOA system; reported in Paper I. The results show that when [HF] < about 0.06 M, the extraction sequence is Nb>Ta, when [HF] > about 0.06 M, the extraction sequence changes into Ta>Nb as shown in Fig. 5. 13.

Presumably, at [HF] < about 0.06 M, Ta and Nb form preferably sulphuric or bisulphate complexes which dominate over fluoric complexes, and Ta shows a lower extraction efficiency than Nb. With increasing [HF], Ta and Nb form a fluoric complex, the anionic fluoride complexes of Ta being stronger than those of Nb: It is known that Ta is very prone to form various anionic species like $[TaF_6]^-$, $[TaF_7]^{2-}$$[TaF_8]^{3-}$, $[TaF_9]^{4-}$ $[TaOF_5]^{2-}$, $[TaOF_6]^{3-}$ etc. [114, 115] while Nb forms only $[NbF_6]^-$ [116] in hydrofluoric acid medium and shows little tendency to interact with F^- to generate the higher co-ordinated anion or metal oxy-anions.

These complexes dominate over the sulphate and bisulphate complexes. Thus, the preferential extraction of Ta to Nb by TOA may be attributed to the fact that the various Ta metal-anionic and oxy-anionic species bind to the quaternary ammonium salt to a greater extent in comparison to Nb complexes. Experimental results confirm this evaluation.

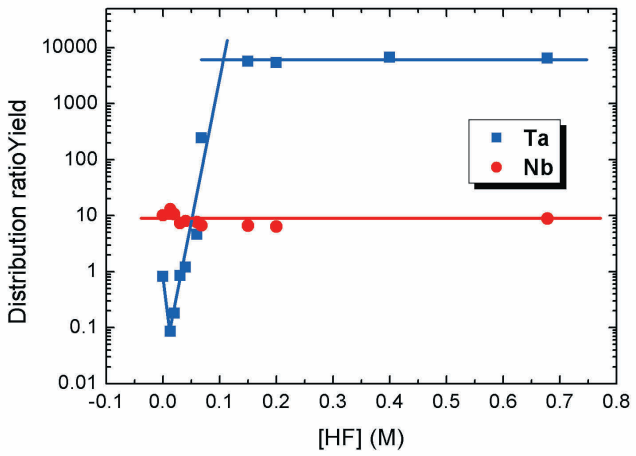

Fig. 5. 13 Variation in the distribution ratio as a function of aqueous HF concentration in 0.5 M H_2SO_4: Batch experiments for Ta and Nb extracted with 0.1 M TOA in toluene

5.1.7 The Extraction of Ta and Nb into Aliquat 336 in Toluene from H_2SO_4 with or without H_2O_2 Present

The ^{175}W tracer was produced together with the 2.36-h ^{178}Ta. When extraction data were processed, those of ^{175}W were also processed and used as reference values, which are shown below.

Fig. 5.13 shows that the sequence is Nb > Ta > W for the extraction with Aliquat 336 in toluene from H_2SO_4 solutions. An increase in the concentration of H_2SO_4 has only a small influence on the distribution ratios for Nb, but these ratios for both Ta and W decrease with increasing H_2SO_4 concentrations. The slope of the extraction curve is -0.8 ±0.1 for Ta and -1.3 ± 0.1 for W. The distribution ratios for W are in good agreement with those in the work of Johansson et al. [117], although their data was from batch experiments. The separation factors of Nb/Ta are 1.7 at 0.1 M H_2SO_4 and 10.5 at 1.0 M H_2SO_4 (see Table 5.5).

A characteristic feature of the Group-5 elements is the formation of hydrophilic peroxide complexes [118]. Broden et al. added hydrogen peroxide to the aqueous solution to

form a complex with Nb. This effectively suppressed its extraction into Alamine 336 in Shellsol-T, but did not influence the extraction of Zr. Thus, the addition of H_2O_2 enables effective extraction of Zr from Nb. Our investigation in utilizing Aliquat 336 for the extraction of Nb and Ta also includes the use of H_2O_2 in complex formation with these homologues.

Based on the results obtained from the kinetics experiments with H_2SO_4/Aliquat 336 in toluene and with H_2SO_4/TOA in toluene it was decided that 43-mm length is sufficient to reach the extraction equilibrium for both Ta and Nb at a 0.4 ml/s flow rate.

As the extraction of Ta decreases with the H_2SO_4 concentration, the competition between sulphate ions and anionic metal species for association with cationic $R^1R^2R^3CH_3N^+$ (R_4N^+) are presumable, but also the possible formation of less readily extractable complexes. The effect of the bisulphate ions can be disregarded due to the lower affinity of HSO_4^- towards the quaternary ammonium ion compared to Cl^-.

With increasing H_2SO_4 concentration the distribution ratio of Nb is constant. Thus, the formed neutral species dominates over the anion species in solutions and the value of the distribution ratio is equal to the partition ratio of a probable $Nb(OH)(SO_4)_2$ complex added to Aliquat 336 sulphate (see Paper II).

Addition of H_2O_2 lowers the extraction of both Ta and Nb, especially of Nb. However, addition of H_2O_2 increases the extraction of W. The extraction sequence is changed into W>Ta>Nb (see Fig. 5.14). The proposed formula of the complex is $Nb(OH)_4(H_2O_2)^+$ [119], which explains that this Nb compound is not extractable with Aliquat 336. Ta forms probably similar species, but to a lesser extent because of its stronger hydrolysis (see Paper II).

With respect to W, the effect of H_2O_2 is enhanced extraction which may be caused by increased formation of anions, or ions having higher affinity to Aliquat 336. It is possible that H_2O_2 bound to W gives off H^+, thus forming a negatively charged complex.

A distinctive change in distribution ratios takes place when the H_2O_2 concentration in the aqueous phase is changed from zero to 0.05 M. Further increase in the H_2O_2 concentration does not make significant changes in the D-values (see Fig. 5.17).

At 0.1 M H_2SO_4 with 1.0 M H_2O_2, the separation factor of Ta and Nb is 6, and the distribution ratios of Nb and Ta are 0.18 and 1.06, respectively. These should be suitable conditions for exploring possible hydrogen peroxide complex formation with Db in SISAK experiments.

Fig. 5.15 shows γ-ray spectra obtained from organic phase in the extraction of Nb from 1.0 M H_2SO_4 into 0.1 M Aliquat 336 and the extraction from 1.0 M H_2SO_4 with 1.0 M H_2O_2 present into 0.1 M Aliquat 336. γ-lines of different radionuclides of Nb were observed and labelled. As seen from (b), almost all Nb peaks compared to (a) disappeared upon the addition of H_2O_2, which means the extraction of Nb was greatly suppressed by H_2O_2.

Fig. 5.16 shows γ-ray spectra obtained from organic phase in the extraction of Ta from 0.1 M H_2SO_4 into 0.1 M Aliquat 336 and the extraction of Ta from 0.1 M H_2SO_4 with 1.0 M H_2O_2 present into 0.1 M Aliquat 336. γ-lines of different radionuclides of Ta and W were observed and labelled. As seen from (a) and (b), the effect of H_2O_2 on the extraction of Ta is not as strong as it is on the extraction of Nb.

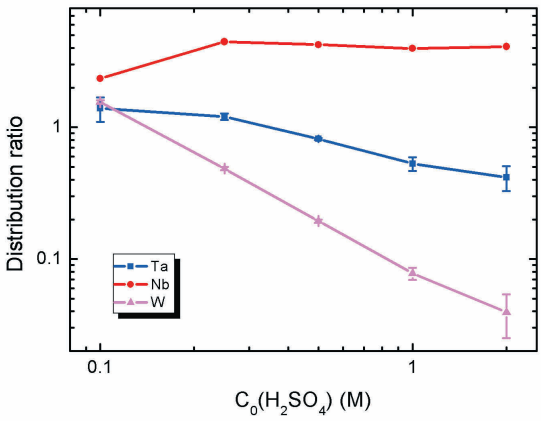

Fig. 5. 14 Results from SISAK on-line extraction of Nb, Ta and W from various H_2SO_4 concentrations into 0.1 M Aliquat 336 in toluene. C_0 is initial H_2SO_4 concentration.

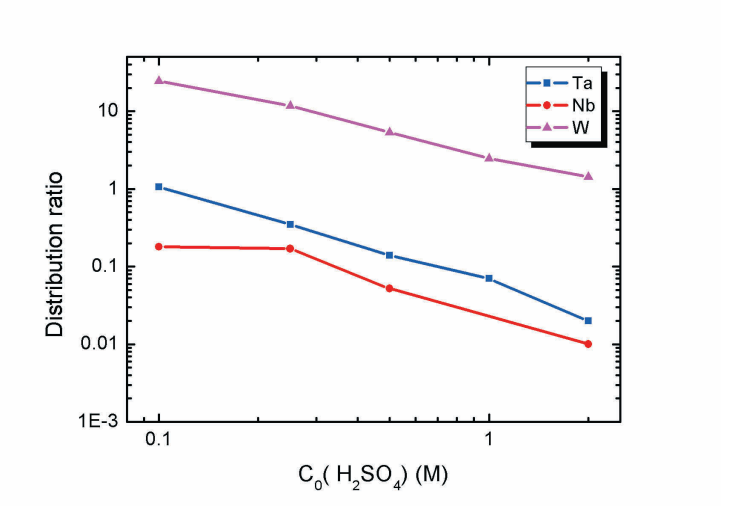

Fig. 5. 15 Results from SISAK on-line extraction of Nb, Ta and W from various H_2SO_4 concentrations containing 1.0 M H_2O_2 into 0.1 M Aliquat 336 in toluene. The H_2O_2 introduced into the degasser along with the H_2SO_4 at around 80 ºC.

Table 5. 5 Distribution ratios and separation factors of Nb/Ta (SF) with 0.10 M Aliquat 336 in toluene from various H_2SO_4 concentrations with or without 1.0 M H_2O_2

H_2SO_4 (M)	Without H_2O_2			With H_2O_2		
	D(Ta)	D(Nb)	SF	D(Ta)	D(Nb)	SF
0.1	1.39	2.35	1.7	1.06	0.18	6
0.25	1.2	4.46	3.7	0.35	0.17	2
0.5	0.82	4.24	5.2	0.14	0.05	3
1	0.38	3.97	10.5	0.07	---	---
2	0.42	4.1	9.8	0.02	0.01	2

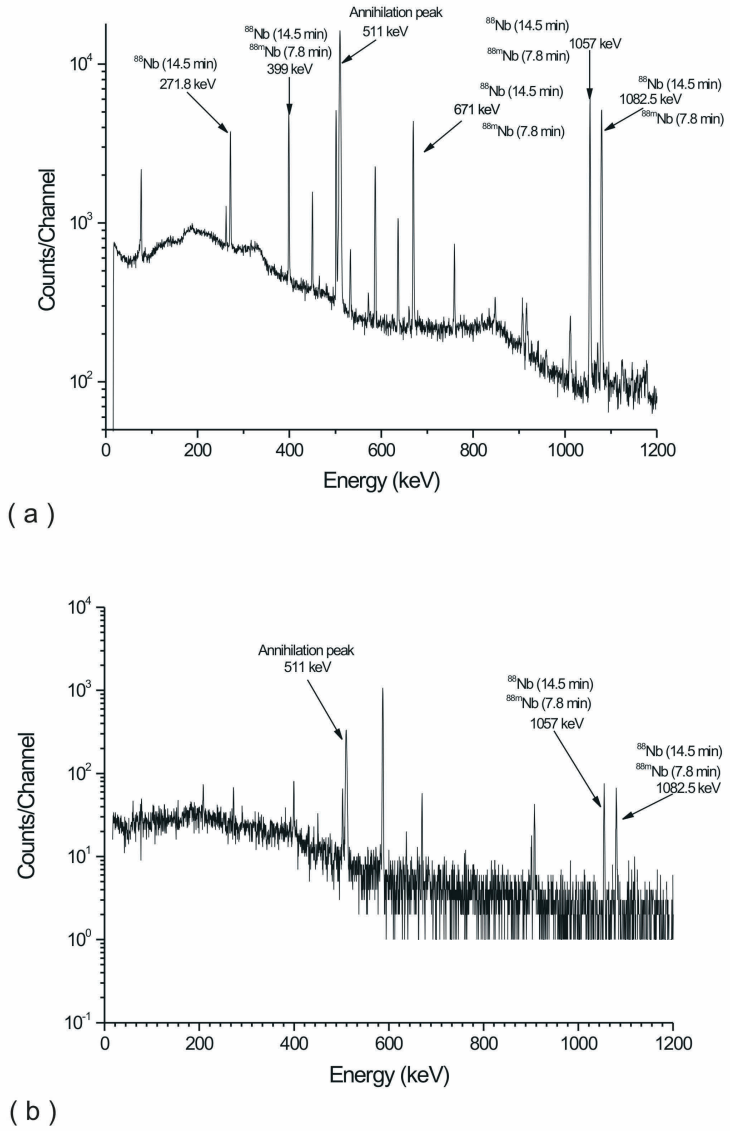

Fig. 5. 16 γ-ray spectra obtained from organic phase in the extraction of Nb from 1.0 M H_2SO_4 into 0.1 M Aliquat 336 (a)and the extraction from 1.0 M H_2SO_4 with 1.0 M H_2O_2 present into 0.1 M Aliquat 336 (b) in the reaction $^{3}He + {}^{nat89}Y$ used for production of ^{88}Nb (T ½ =14.5 min) and ^{88m}Nb (T ½ =7.8 min). Acquisition of the spectra was started after a 7-min sampling and a 1-min gap. Measuring time was 9 min. γ-lines of different radionuclides of Nb were observed and labelled. As seen from (b), almost all Nb peaks compared to (a) disappeared upon the addition of H_2O_2, which means the extraction of Nb was greatly suppressed by H_2O_2.

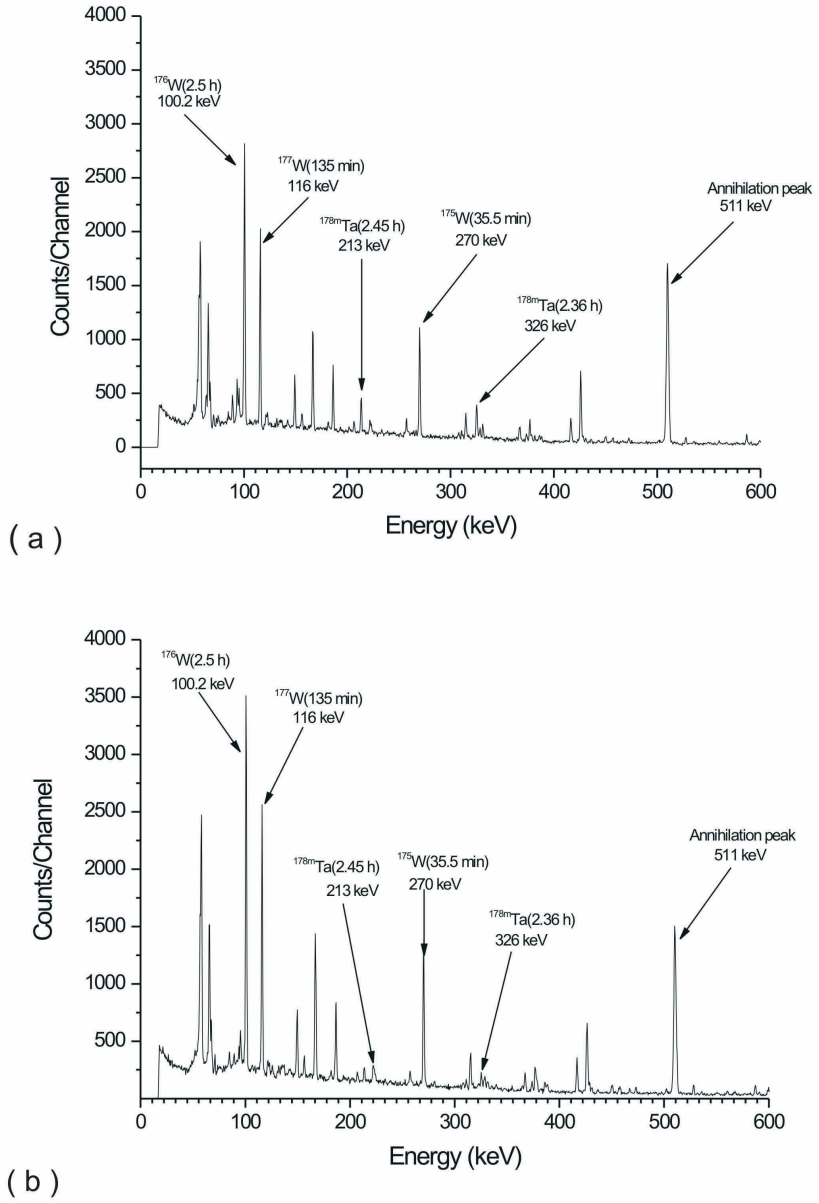

Fig. 5. 17 γ-ray spectra obtained from organic phase in the extraction of Ta from (a) 0.1 M H_2SO_4 into 0.1 M Aliquat 336 and (b) the extraction of Ta from 0.1 M H_2SO_4 with 1.0 M H_2O_2 present into 0.1 M Aliquat 336 in the reaction $^{3}He + {}^{nat}Hf$ used for production of ^{178}Ta (T ½ =2.45 h). Acquisition of the spectra was started after a 7-min sampling and a 1-min gap. Measuring time was 9 min. γ-lines of different radionuclides of Ta and W were observed and labelled. As seen from (a) and (b), the effect of H_2O_2 on the extraction of Ta is not as strong as it is on the extraction of Nb.

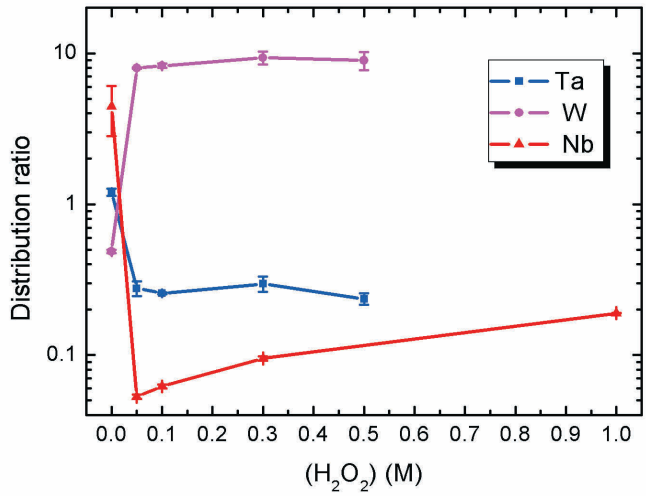

Fig. 5. 18 SISAK on-line extraction of Nb,Ta and W from various concentrations of H_2O_2 present in 0.25 M H_2SO_4 solution with 0.1 M Aliquat 336 in toluene.

5.2 Influence of KCl from Gas-jet on the Extraction

In studies of the extraction chemistry of Rf produced by the reaction $^{208}Pb(^{50}Ti,n)^{257}Rf$, the radionuclide is separated from other reaction products in a gas separator (BGS) and recoils into the RTC chamber from which it is transferred to the SISAK liquid-liquid extraction system by a He gas-jet. The He gas-jet contains potassium chloride aerosol particles in order to carry and transport reaction products to the SISAK system. Attached to KCl aerosols in the He gas-jet the activity is dissolved in the aqueous phase by means of a stationary mixer. Inevitably, the potassium chloride enters the aqueous phase also. Due to the high amounts of liquid consumed by the SISAK system during transactinide experiments, which typically last several days, recycling of chemicals is necessary in order to reduce chemicals expense and the amount of waste. This results in build-up of KCl in the aqueous phase. Under the extraction conditions given, the possible interference from the KCl aerosol on the extraction of Rf was examined by determining the influence of KCl on the distribution ratios of Zr and Hf in the H_2SO_4/TOA system. The detailed description of this investigation is presented in Paper III.

The investigation shows that the distribution ratios of both Hf and Zr decrease with the addition of KCl, that of Hf somewhat more than that of Zr. A possible explanation is that the chloride ions compete with bisulphate ions and form $(R_3NH)Cl$ ion pairs which may not extract zirconium and hafnium. There is a small difference in the effect in the sequence observed: HCl < LiCl < KCl.

In additional research on this subject, it was found that the reduction in distribution ratio with addition of LiCl is almost the same as for KCl within statistical uncertainty. This indicates that there should be no interference in the extraction from K^+ ions but only from Cl^- ions. Adding HCl, however, increases the H^+ concentration and favours the amine bisulphate formation, which in turn counteracts the Cl^- effect to some extent. Subsequently, the reduction in the distribution ratio with addition of HCl is somewhat less than that for addition of KCl or LiCl. Thus, the sequence in the effect should be: HCl < LiCl = KCl.

Any distinct effect from KCl in the gas-jet on the extraction should not appear as long as the accumulated Cl^- concentration due to recycling of aqueous phase during transactinide SISAK experiments is kept below 10^{-3} M.

5.3 SISAK Rutherfordium Experiments

In the 2003 experiment, after correction for the decay loss of 4.7 s ^{257}Rf, gas-jet yield equal to 50% for transfer to scintillator solution and 67% for transfer to heated aqueous solution, it is possible to calculate the expected number of correlation events in the detectors: with 100% yield in the extraction stage, one αα-correlation is expected in detector cell 1 for 70.2k counts in the Rutherford scattering detectors. Thus, for detector cell 1, with 529k scattering counts, about 7.5 correlations are expected if the extraction is 100% (see Table 2 in Paper IV).

For the number of expected correlations in detector 2, it is assumed that detector cell 1 always is open and the activity is delayed by about one half-life before it reaches cell 2. Thus, only one correlation per 140.4k counts is expected in cell 2.

Of the 32 events which closed cell 1, a possible daughter was observed in only 13. Three are disregarded due to energy above 12 MeV (two cases) or energy below 7.5 MeV (one case); see Figure 5 and Table 4 in Paper 4. For detector 1, five correlations compared to the 7.5 correlations expected indicate that 2.5 correlations must be assumed to have remained in the aqueous phase. Taking the flow rates of the two phases into account, these results in a distribution value, D, equal to 2.2. Since the uncertainty in the transport time, gas-jet yield, the degasser yield, etc. are difficult to estimate, the uncertainty of this D value is large and difficult to calculate. The large uncertainty due to the many parameters in the equation to calculate the activity in the aqueous phase clearly indicates that a more accurate method is highly desirable. Therefore, such a method, a two-step extraction procedure, was developed and used for the 2005 experiment.

In the 2005 experiment, as shown in Table 5 in Paper 4, the observed number of ^{257}Rf-^{253}No αα correlations in the organic phase for the first detector was two. Twenty-eight events closed the cell, but a daughter was observed in only five cases. Only three of those had energy within the 8.2-9.3 MeV range expected for ^{257}Rf. One of the three events had too high daughter energy and was rejected, as shown in Figures 6 and Figure 7 in Paper 4.

The number of correlations observed for the second organic phase was 6; this represents the amount of aqueous activity. Twenty-eight events closed the cell; in 12 of these closures a daughter event was observed. Ten of the correlated closures had mother energies within the right range; of these, six had acceptable daughter energies.

The number of correlations in the aqueous phase is estimated to be 13.5. This is based on 6 observed correlations in the first detector for the organic phase in the second extraction step, in which it is assumed that 80% of the ^{257}Rf is extracted, and an additional delay of 4.1 s due to the second extraction step.

The gated integrals, (counts in the the Rutherford-scattering detectors when the alpha-detector cells are "open" are 55 kcounts for the first organic phase and 552 kcounts for the second organic phase. Taking the gated integrals and the flow rate into account, a distribution ratio, D, equal to 0.2 is obtained for extraction with 0.003 M TOA.

The two-step extraction procedure demonstrates the advantage of measuring the activity in both phases simultaneously with direct detection of alpha activity of both organic phases as compared to indirect determination of the amount of activity in the aqueous phase. This simultaneous measurement of activity in the phases increases efficiency since the amount of activity entering the system no longer needs to be measured in a separate experiment. Furthermore, the uncertainty resulting from changing and uncertain yields in the aerosol gas-jet transport of activity from the RTC to the aqueous phase is eliminated.

6 Conclusions

1. The investigation of the extraction system H_2SO_4/TOA demonstrates that:
    i) the extraction kinetics are fast enough concerning decay loss of the nuclides of interest;
    ii) both pure aqueous and organic phases have been achieved;
    iii) the chemicals involved are easy to handle;
    iv) distribution ratios between 0.1 and 10 can be obtained;
    v) the separation factors between Nb and Ta are large enough so that Ta and Nb can be clearly distinguished.

This promising chemistry has been recommended as the chemical extraction system for the Db SISAK experiments to be performed at LBNL, as proposed in the 2007 proposal (see Appendix 6). Due to beam time rescheduling, this experiment was postponed and is now planned for 2008 [REF: Heino Nitsche, personal communication].

At 0.1 M TOA/0.1 M H_2SO_4 with 0.25 M K_2SO_4 present, the D values of Nb and Ta are 0.35 and 3.79, respectively, with a separation factor of around 11. At 0.02 M TOA/0.25 M H_2SO_4, the D values of Nb and Ta are 0.48 and 5.2, respectively, with a separation factor of around 11. These two concentrations should be suitable for Db SISAK transactinide experiments to start with.

If 0.1 TOA/H_2SO_4 with 0.25 M K_2SO_4 system were chosen, the recommended procedures for implementing Db SISAK experiments would be as follows:

a. Starting with 0.1 M H_2SO_4 with 0.25 M K_2SO_4 and 0.1 M TOA by using two-stage extraction setup to measure the D-value of Db.
b. If the measured D-value from the first procedure is between 0.1 and 4, then increase the acid concentration to 0.5 M H_2SO_4 with 0.25 M K_2SO_4 to measure the D-value of Db at this concentration. With the D-values of the two concentrations, the slope of the Db extraction curve can be obtained.
c. If the measured D-value of Db is bigger than 4, then decrease the acid concentration to 0.05 M H_2SO_4 with 0.25 M K_2SO_4 to measure the D-value at this concentration. With the D-values of the two concentrations, the slope of the Db extraction curve can be obtained.

If TOA/0.25 M H_2SO_4 system were chosen, the recommended procedures for Db experiment would be as follows:

a. Starting with 0.02 M TOA by using two-stage setup to measure the D-value of Db
b. If the measured D-value from the first procedure is between 0.1 and 5.2, then increase the extraction agent concentration to 0.1 M TOA to measure the D-value of Db at this concentration. With the D-values of the two concentrations, the slope of the Db extraction curve can be obtained.
c. If the measured D-value is bigger than 5.2, then decrease the extraction agent concentration to 0.01 M TOA and measure the D-value of Db at this concentration. With the D-values of the two concentrations, the slope of the Db extraction curve can be obtained.

One might be able to judge whether Db is Nb-like or Ta-like by comparing the slope of the Db curve with the ones for Ta and Nb curves.

2. Under Aliquat 336 in toluene/H_2SO_4 system, at 0.1 M H_2SO_4 with 1.0 M H_2O_2, the separation factor of Ta and Nb is 6, and the distribution ratios of Nb and Ta are 0.18 and 1.06, respectively. These should provide suitable conditions for exploring possible hydrogen peroxide complex formation with Db in SISAK experiments. Based on the theoretical calculations by V. Pershina [120] of the hydrolysis of

compounds of Group-5 elements with increasing HCl concentration, the hydrolysis of complexes decreases in the order

Ta > Db > Nb > Pa.

If this is the sequence also for sulphate complexes of Group-5 homologues and if peroxide complexes are formed, the distribution ratios of Db would be expected to be between those of Ta and Nb.

3. The two Rf SISAK experiments demonstrate the advantage of measuring the activity in both phases simultaneously using a two-step extraction procedure with direct detection of alpha activity of both organic phases as compared to indirect determination of the amount of activity in the aqueous phase. This simultaneous measurement of activity in the phases increases efficiency since the amount of activity entering the system no longer needs to be measured in a separate experiment. Furthermore, the uncertainty resulting from changing and uncertain yields in the aerosol gas-jet transport of activity from the RTC to the aqueous phase is eliminated. Moreover, Setup C in Fig. 3.3 establishes the way in which future SISAK transactinide experiments will be performed and enables the SISAK system to be used for dubnium or even heavier elements.

Future Perspective

1. SISAK extraction schemes can be developed to focus on the chemical properties within one periodic group. It would be ideal to study a transacinide element when its homologues are produced and investigated simultaneously. The utilization of a heavy-ion “cocktail” allows for such chemical investigation of preseparated TAEs and their periodic table homologues under identical conditions. For example, the Group-5 elements Nb, Ta and Db can be produced with a $^{18}O^{5+}/^{51}V^{14+}$ cocktail using the reactions $^{74}Se(^{18}O,pxn)^{87,88}Nb$, $^{112,116,120,124}Sn(^{51}V,xn)^{160-171}Ta$ and $^{209}Bi(^{51}V,n)^{259}Db$ [121].
2. The Pre-separator BGS has made the chemistry experiments with SISAK greatly profit from a strongly reduced background and more “chemistry-friendly”

conditions. The BGS is most efficient for nuclides produced in fusion reactions between Z ~ 20 accelerated particles onto targets of Pb/Bi. Another recoil separator designed for Superheavy-element chemistry, namely TASCA (TransActinide Separator and Chemistry Apparatus), is currently under construction at the GSI UNILAC facility in Germany. The TASCA separator is being designed to enable the use of Pu targets. This has previously not been possible at BGS due to concerns regarding safety and maintaining a low-level detection environment. With the TASKA facility, relatively long-lived nuclides of Db isotopes will become accessible for SISAK Db chemistry experiments. For example, the 33-s ^{262}Db from the reaction ^{244}Pu(^{23}Na,5n)^{262}Db (with 32% decay loss in SISAK, which is much less than that for the ^{257}Rf used in SISAK Rf experiments), can penetrate up to a 1.9 μm Mylar RTC window with 10.8 EVR recoil energy [17]. A new RTC-window design is being developed for TASCA [122, 123] which will enable much thinner windows than those that have been used at the BGS so far. A similar window construction should also be possible for the BGS. Thus, chemistry studies with EVRs from Pu-targets should be possible at both separators in the near future.

3. Single atom chemistry and detection with the current set-up of SISAK coupled to the BGS is optimum for nuclides of half-lives in the range of ~ 4 to 30 seconds. Detection of nuclides with longer half-lives, e.g., ^{262}Db with a half-life of 33 s, can be achieved with additional detection cells, but a detection cell and the analogue electronic modules are an expensive investment. Further development of the detection cell should result in a larger hold-up volume.

References

1. Mendeleev, D., Z. Chem. **12**, 405 (1869).
2. Mendeleev, D., Liebigs, A., Chem. Supplementband **7**, 133 (1871).
3. Gregorich, K. E.: *Radiochemistry of rutherfordium and hahnium*, in proceedings from *The Robert A. Welch Foundation Conference on Chemical Research, 41st 95-124. CODEN: PRAWAC*, Taxas, 1997, ed.), ISBN 0557-1588. CAN 128:276038 AN 1998:182759 CAPLUS,
4. Seaborg, G. T., in *Handbook on the Physics and Chemistry of Rare Earths*, 1994), Vol. 18, p. 1.
5. Seaborg, G. T., Journal of the Chemical Society-Dalton Transactions, 3899 (1996).
6. Eberhardt, K., Alstad, J., Brüchle, W., et al., Jahresbericht, Institut für Kernchemie, Universität Mainz (1995).
7. Nagame, Y., Haba, H., Tsukada, K., Asai, M., Toyoshima, A., Goto, S., Akiyama, K., Kaneko, T., Sakama, M., Hirata, M., Yaita, T., Nishinaka, I., Ichikawa, S., and Nakahara, H., Nucl. Phys. A **734**, 124 (2004).
8. Guseva, L. I., Uspe. Khim. **74**, 484 (2005).
9. Eichler, R., Bruchle, W., Dressler, R., et al., Nature **407**, 63 (2000).
10. Pershina, V., Fricke, B., Kratz, J. V., Ionova, G. V., Radiochim. Acta **64**, 37 (1994).
11. Omtvedt, J. P., Polakova, D., Alstad, J., et al.: *Study of Liquid-liquid Extraction of Element 104, Rutherfordium-Sulphate Complexes by the SISAK System*2007, to be published.
12. Oganessian, Y. T., Radiat. Phys. Chem. **61**, 259 (2001).
13. Munzenberg, G., Radiochim. Acta **70-1**, 193 (1995).
14. Munzenberg, G., Hofmann, S., Folger, H., Hessberger, F. P., Keller, J., Poppensieker, K., Quint, B., Reisdorf, W., Schmidt, K. H., Schott, H. J., Armbruster, P., Leino, M. E., and Hingmann, R., Zeitschrift Fur Physik a-Hadrons and Nuclei **322**, 227 (1985).
15. Malmbeck, R., Ph.D thesis: *Applications of On-line Continuous Solvent Extraction in Nuclear Chemistry,* Department of Nuclear Chemistry, Chalmers University of Technology Göteborg Sweden, 1997.
16. Omtvedt, J. P., Alstad, J., Hanne, B., et al., J. Nucl. Radiochem. Sci. **3**, 121 (2002).
17. Omtvedt, J. P., Alstad, J., Bjørnstad, T., Düllmann, C. E., III, C. M. F., Gregorich, K. E., Hoffman, D. C., Nitsche, H., Polalova, D., Samadani, F., Skarnemark, G., Stavsetra, L., Sudowe, R., and Zheng, L.: *SISAK Liquid-liquid Extraction Studies of Rutherfordium and Future Plans to Study Heavier Transactinides*, in proceedings from *Recent Advances in Actinide Science*, University of Manchester, UK, 2006

(May, I., Alvares, R., Bryan, N. d. , ed.), Royal Society of Chemistry, CODEN: SROCDO, ISBN 0260-6291. AN 2006:1125374 CAPLUS
18. Hoffman, D. C., Radiochim. Acta **61**, 123 (1993).
19. Hoffman, D. C., Radiochim. Acta **72**, 1 (1996).
20. Mathhias, S., *The Chemistry of Superheavy Elements* (kluwer Academic Publishers, Gesellschaft für Schwerionenforschung mbH (GSI), Darmstadt, Germany, 2003).
21. Silva, R., Harris, J., Nurmia, M., Eskola, K., and Ghiorso, A., Inorganic & Nuclear Chemistry Letters **6**, 871 (1970).
22. Szeglowski, Z., Bruchertseifer, H., Domanov, V. P., Gleisberg, B., Guseva, L. J., Hussonnois, M., Tikhomirova, G. S., Zvara, I., and Oganessian, Y. T., Radiochim. Acta **51**, 71 (1990).
23. Pfrepper, G., Pfrepper, R., Krauss, D., Yakushev, A. B., Timokhin, S. N., and Zvara, I., Radiochim. Acta **80**, 7 (1998).
24. Strub, E., Kratz, J. V., Kronenberg, A., et al., Radiochim. Acta **88**, 265 (2000).
25. Haba, H., Tsukada, K., Asai, M., et al., J. Nucl. Radiochem. Sci. **3**, 143 (2002).
26. Haba, H., Tsukada, K., Asai, M., et al., J. Amer. Chem. Soc. **126**, 5219 (2004).
27. Kronenberg, A., Eberhardt, K., Kratz, J. V., Mohapatra, P. K., Nahler, A., Thorle, P., Bruchle, W., Schadel, M., and Turler, A., Radiochim. Acta **92**, 379 (2004).
28. Hulet, E. K., Lougheed, R. W., Wild, J. F., Landrum, J. H., Nitschke, J. M., and Ghiorso, A., J. Inorg. Nucl. Chem. **42**, 79 (1980).
29. Gunther, R., Paulus, W., Kratz, J. V., et al., Radiochim. Acta **80**, 121 (1998).
30. Czerwinski, K. R., Kacher, C. D., Gregorich, K. E., Hamilton, T. M., Hannink, N. J., Kadkhodayan, B. A., Kreek, S. A., Lee, D. M., Nurmia, M. J., Turler, A., Seaborg, G. T., and Hoffman, D. C., Radiochim. Acta **64**, 29 (1994).
31. Czerwinski, K. R., Gregorich, K. E., Hannink, N. J., Kacher, C. D., Kadkhodayan, B. A., Kreek, S. A., Lee, D. M., Nurmia, M. J., Turler, A., Seaborg, G. T., and Hoffman, D. C., Radiochim. Acta **64**, 23 (1994).
32. Kadkhodayan, B., Turler, A., Gregorich, K. E., et al., Radiochim. Acta **72**, 169 (1996).
33. Kacher, C. D., Gregorich, K. E., Lee, D. M., et al., Radiochim. Acta **75**, 127 (1996).
34. Bilewicz, A., Siekierski, S., Kacher, C. D., Gregorich, K. E., Le, D. M., Stoyer, N. J., Kadkhodayan, B., Kreek, S. A., Lane, M. R., Sylwester, E. R., Neu, M. P., Mohar, M. F., and Hoffman, D. C., Radiochim. Acta **75**, 121 (1996).
35. Gregorich, K. E., Henderson, R. A., Lee, D. M., Nurmia, M. J., Chasteler, R. M., Hall, H. L., Bennett, D. A., Gannett, C. M., Chadwick, R. B., Leyba, J. D., Hoffman, D. C., and Herrmann, G., Radiochim. Acta **43**, 223 (1988).
36. Zimmermann, H. P., Gober, M. K., Kratz, J. V., et al., Radiochim. Acta **60**, 11 (1993).
37. Kratz, J. V., Zimmermann, H. P., Scherer, U. W., et al., Radiochim. Acta **48**, 121 (1989).
38. Gober, M. K., Kratz, J. V., Zimmermann, H. P., et al., Radiochim. Acta **57**, 77 (1992).
39. Paulus, W., Kratz, J. V., Strub, E., et al., Radiochim. Acta **84**, 69 (1999).
40. Schadel, M., Bruchle, W., Schimpf, E., et al., Radiochim. Acta **57**, 85 (1992).
41. Trubert, D., Le Naour, C., Guzman, F. M., Hussonnois, M., Brillard, L., Le Du, J. F., Constantinescu, O., Gasparro, J., Barci, V., Weiss, B., and Ardisson, G., Radiochim. Acta **90**, 127 (2002).
42. Kratz, J. V., Nahler, A., Rieth, U., et al., Radiochim. Acta **91**, 59 (2003).
43. Schadel, M., Bruchle, W., Schausten, B., et al., Radiochim. Acta **77**, 149 (1997).

44. Schadel, M., Bruchle, W., Jager, E., et al., Radiochim. Acta **83**, 163 (1998).
45. Aronsson, P. O., Johansso.Be, Rydberg, J., Skarnema.G, Alstad, J., Bergerse.B, Kvale, E., and Skaresta.M, J. Inorg. Nucl. Chem. **36**, 2397 (1974).
46. Persson, H., Skarnemark, G., Skalberg, M., Alstad, J., Liljenzin, J. O., Bauer, G., Haberberger, F., Kaffrell, N., Rogowski, J., and Trautmann, N., Radiochim. Acta **48**, 177 (1989).
47. Tetzlaff, H., Herrmann, G., Kaffrell, N., et al., J. Less-Common Met. **122**, 441 (1986).
48. Skålberg, M., Ph.D thesis: *Rapid Chemical Separations Applied in Nuclear Research,* Dept. of Nuclear Chemistry, Chalmers University of Technology, 1991.
49. Wierczinski, B., Gregorich, K. E., Kadkhodayan, B., et al., J. Radioanal. Nucl. Chem. **247**, 57 (2001).
50. Wierczinski, B., Ph.D thesis thesis: *Untersuchung zur Extraktion der Elemente 105 und 106 mit SISAK 3 und on-line α-Flüssigszintillationsspektroskopie*, University of Mainz, 1994.
51. Wierczinski, B., Eberhardt, K., Herrmann, G., Kratz, J. V., Mendel, M., Nahler, A., Rocker, F., Tharun, U., Trautmann, N., Weiner, K., Wiehl, N., Alstad, J., and Skarnemark, G., Nucl. Instrum. Meth. Phys. Res. **370**, 532 (1996).
52. K. Eberhardt, J. Alstad, H. O. Kling, J. V. Kratz, G. Langrock, J. P. Omtvedt, G. Skarnemark, L. Stavsetra, U. Tharun, N. Trautmann, N. Wiehl, and Wierczinski, B.: *Digital pulse shape analysis in liquid scintillation measurements after continuous chemical separations.*, in proceedings from *Advances in Liquid Scintillation Spectrometry* Karlsruhe, Germany, 2001, 2002, ed.), p. 19, ISBN CODEN: 69FLIZ CAN 141:306487 AN 2004:426955 CAPLUS, p.19
53. K. Eberhardt, J. Alstad, H. Breibik, et al., Jahresbericht, Institut für Kernchemie, Universität Mainz. (2000).
54. K. Eberhardt, J. Alstad, W. Brüchle, et al., Jahresbericht, Institut für Kernchemie, Universität Mainz (1998).
55. K. Eberhardt, J. Alstad, K. Future, H. W. Gäggeler, M. Gärtner, D. Jost, R. Malmbeck, M. Mendel, A. Nähler, J. P. Omtvedt, G. Skarnemark, N. Trautmann, A. Tüler, and N. Wiehl, Jahresbericht, Institut für Kernchemie, Universität Mainz. (1997).
56. K. Eberhardt, J. Alstad, B. Eichler, et al., Jahresbericht, Institut für Kernchemie, Universität Mainz (1996).
57. McDowell, W. J. and McDowell, B. L., *Liquid Scintillation Alpha Spectrometry* (CRC, Boca Raton, Fla., Florida, 1994).
58. Stevenson, P. C. and Hicks, H. G., Anal. Chem. **25**, 1517 (1953).59. Zvara, I., Belov, V. Z., Domanov, V. P., and Shalaevskii, M. R., Sov. Radiochem. **18**, 328 (1976).
60. Zvara, I., Eichler, B., Belov, V. Z., Zvarova, T. S., Korotkin, Y. S., Shalaevskii, M. R., Shchegolev, V. A., and Hussonnois, M., Sov. Radiochem. **16**, 709 (1974).
61. Hyde, E. K., Hoffman, D. C., and Keller, O. L., Radiochim. Acta **42**, 57 (1987).
62. Keller, O. L. and Seaborg, G. T., Annual Review of Nuclear and Particle Science **27**, 139 (1977).
63. Milner, G. W. C., Barnett, G. A., and Smales, A. A., Analyst **80**, 380 (1955).
64. Werning, J. R., Higbie, K. B., Grace, J. T., Speece, B. F., and Gilbert, H. L., Industrial and Engineering Chemistry **46**, 644 (1954).
65. Desclaux, J. P., At. Data Nucl. Data Tables **12**, 311 (1973).
66. Pershina, V. and Bastug, T., Radiochim. Acta **84**, 79 (1999).
67. Paulus, W., Kratz, J. V., Strub, E., et al., J. Alloy. Comp. **271**, 292 (1998).

68. Maskow, M. P., Ph.D thesis: *Schnelle chemische Trennverfahren mit Zentrifugensystem SISAK 3 zur Untersuchung der Elemente 104,105 und 106*, University of Mainz, 1994.
69. Wierczinski, B., Alstad, J., Eberhardt, K., Eichler, B., Gaggeler, H., Herrmann, G., Jost, D., Nahler, A., Pensemaskow, M., Reddy, A. V. R., Skarnemark, G., Trautmann, N., and Turler, A., Radiochim. Acta **69**, 77 (1995).
70. Stavsetra, L., Ph.D thesis: *Achievements using the continuous SISAK α-liquid scintillation technique, and its application in detection of ^{257}Rf atoms,* The Department of Chemistry, The University of Oslo, 2005.
71. Marcus, J., Ph.D thesis: *Radiochemical Separation Systems adapted for Studying Transactinide Chemistry with SISAK*, The University of Oslo, 2000.
72. Hessberger, F. P., Munzenberg, G., Hofmann, S., Reisdorf, W., Schmidt, K. H., Schtt, H. J., Armbruster, P., Hingmann, R., Thuma, B., and Vermeulen, D., Zeitschrift Fur Physik a-Hadrons and Nuclei **321**, 317 (1985).
73. G. Pfennig, H. Klewe-Nebenius, and W. Seelmann-Eggebert, Karlsruher Nuklidkarte, 6. Auflage Korrigerte Nachdruck, Forschungszentrum Karlsruhe, Germany (1998).
74. Hofmann, S., Hessberger, F. P., Ninov, V., Armbruster, P., Munzenberg, G., Stodel, C., Popeko, A. G., Yeremin, A. V., Saro, S., and Leino, M., Zeitschrift Fur Physik a-Hadrons and Nuclei **358**, 377 (1997).
75. Ghiorso, A., Nurmia, M., Harris, J., Eskola, K., and Eskola, P., Phys. Rev. Lett. **22**, 1317 (1969).
76. Bemis, C. E., Silva, R. J., Hensley, D. C., Keller, O. L., Tarrant, J. R., Hunt, L. D., Dittner, P. F., Hahn, R. L., and Goodman, C. D., Phys. Rev. Lett. **31**, 647 (1973).
77. Ghiorso, A., Nurmia, M., Eskola, K., and Eskola, P., Phys. Lett. B **32**, 95 (1970).
78. Münzenberg, G., Hofmann, S., Folger, H., Hessberger, F. P., Keller, J., Poppensieker, K., Quint, B., Reisdorf, W., Schmidt, K. H., Schott, H. J., Armbruster, P., Leino, M. E., Hingmann, R., Zeitschrift Fur Physik a-Hadrons and Nuclei **322**, 227 (1985).
79. Wilk, P. A., Gregorich, K. E., Hendricks, M. B., Lane, M. R., Lee, D. M., McGrath, C. A., Shaughnessy, D. A., Strellis, D. A., Sylwester, E. R., and Hoffman, D. C., Phys. Rev. C **58**, 1352 (1998).
80. Ghiorso, A., Nurmia, M., Eskola, K., and Eskola, P., Phys. Rev. C **4**, 1850 (1971).
81. Kratz, J. V., Gober, M. K., Zimmermann, H. P., et al., Phys. Rev. C **45**, 1064 (1992).
82. Bemis, C. E., Ferguson, R. L., Plasil, F., Silva, R. J., Okelley, G. D., Kiefer, M. L., Hahn, R. L., Hensley, D. C., Hulet, E. K., and Lougheed, R. W., Phys. Rev. Lett. **39**, 1246 (1977).
83. Lazarev, Y. A., Lobanov, Y. V., Oganessian, Y. T., et al., Phys. Rev. Lett. **73**, 624 (1994).
84. Lougheed, R. W., Moody, K. J., Wild, J. F., et al., J. Alloy. Comp. **213/214**, 61 (1994).
85. Turler, A., Dressler, R., Eichler, B., Gaggeler, H. W., Jost, D. T., Schadel, M., Bruchle, W., Gregorich, K. E., Trautmann, N., and Taut, S., Phys. Rev. C **57**, 1648 (1998).
86. Wilk, P. A., Gregorich, K. E., Turler, A., et al., Phys. Rev. Lett. **85**, 2697 (2000).
87. Turler, A., Dullmann, C. E., Gaggeler, H. W., et al., Europ. Phys. J. A **17**, 505 (2003).
88. Wollnik, H., Nucl. Instrum. Meth. **137**, 169 (1976).
89. Talbert, W. L., Bunker, M. E., and Starner, J. W., Nuc. Instr. Meth. in Phys. Rec. B **26**, 345 (1987).
90. Türler, A., in *Scientific report 0174-0814*, Darmstadt, Germany, 1996).
91. Gaggeler, H. W., J. Radioanal. Nucl. Chem. A. **183**, 261 (1994).

92. Trautmann, N., Aronsson, P. O., Björnstad, T., Kaffrell, N., Kvåle, E., Skarestad, M., Skarnemark, G., and Stender, E., Inorg. Nucl. Chem. Lett. 11, 729 (1975).
93. Hickmann, U., Greulich, N., Trautmann, N., Gaggeler, H., Gaggelerkoch, H., and Eichler, B., Nucl. Instrum. Meth. **174**, 507 (1980).
94. Zvara, I., Isotopenpraxis **26**, 251 (1990).
95. Gaggeler, H. W., Jost, D. T., Kovacs, J., et al., Radiochim. Acta **57**, 93 (1992).
96. Turler, A., Gaggeler, H. W., Gregorich, K. E., et al., Journal of Radioanalytical and Nuclear Chemistry-Articles **160**, 327 (1992).
97. Schadel, M., Bruchle, W., Dressler, R., et al., Nature **388**, 55 (1997).
98. Hoffman, D. C., Lee, D., Ghiorso, A., Nurmia, M. J., Aleklett, K., and Leino, M., Phys. Rev. C **24**, 495 (1981).
99. Gaggeler, H. W., Jost, D. T., Baltensperger, U., Weber, A., Kovacs, A., Vermeulen, D., and Turler, A., Nuc. Instr. Meth. in Phys. Rec. A **309**, 201 (1991).
100. Schadel, M., Bruchle, W., Jager, E., Schimpf, E., Kratz, J. V., Scherer, U. W., and Zimmermann, H. P., Radiochim. Acta **48**, 171 (1989).
101. Paulus, W., Kratz, J. V., Strub, E., et al., Czechoslovak Journal of Physics **49**, 573 (1999).
102. Guzman, M., Ph.D thesis: *Comportement á l'échelle des indicateursdes elements Zr, Hf et 104, Nb et Pa (105) en milieux trèscomplexants*, Université de Paris XI-Orsay, 1997.
103. Trubert, D., Hussonnois, M., Brillard, L., Barci, V., Ardisson, G., Szeglowski, Z., and Constantinescu, O., Radiochim. Acta **69**, 149 (1995).
104. Trubert, D., Hussonnois, M., Le Naour, C., Brillard, L., Guzman, F. M., Le Du, J. F., Servajean, V., Barci, V., Weiss, B., Ardisson, G., Constantinescu, O., and Oganessian, Y., Comptes Rendus De L Academie Des Sciences Serie Ii Fascicule C-Chimie **1**, 643 (1998).
105. Reinhardt, H., Ph.D thesis: *En kontinuerlig separator för två-fas vätskeblandingar*, Chalmers University of Technology 1973.
106. Rydberg, J., Persson, H., Aronsson, P. O., Selme, A., and Skarnemark, G., Hydrometallurgy **5**, 273 (1980).
107. Stavsetra, L., Hult, E. A., and Omtvedt, J. P., Nuc. Instr. Meth. in Phys. Rec. A **551**, 323 (2005).
108. Firestone, R. B. and Shirley, V. S., Nuclear Energy-Journal of the British Nuclear Energy Society **36**, 401 (1997).
109. Poláková, D., Alstad, J., Bjørnstad, T., Opel, K., and Omtvedt, J. P.: *Measurement of Transport Times through the Continuous Liquid-Liquid Extraction System SISAK*, University of Oslo, 2006, to be published.
110. Schafer, H., Angewandte Chemie-International Edition **71**, 153 (1959).
111. Sato, T. and Watanabe, H., J. Inorg. Nucl. Chem. **36**, 2585 (1974).
112. Weast, R. C., *CRC Handbook of chemistry and physics, edition 64*, 1983-1984).
113. Das, N. R. and Lahiri, S., Analytical Sciences **8**, 317 (1992).
114. F. A. Cotton and G. Wilkinson, Advanced Inorganic Chemistry, Wiley Eastern Private Limited, New Delhi, 922 (1969).
115. Martell, A. E. and Gunnar, S. L., *Stability Constants of Metal-Ion Complexes*, 1964).
116. Packer, K. J. and Muetterties, E. L., J. Amer. Chem. Soc. **85**, 3035 (1963).
117. Johansson, M., Alstad, J., Omtvedt, J. P., and Skarnemark, G., Radiochim. Acta **91**, 351 (2003).
118. Broden, K., Skarnemark, G., Bjørnstad, T., Eriksen, D., Haldorsen, I., Kaffrell, N., Stender, E., and Trautmann, N., J. Inorg. Nucl. Chem. **43**, 765 (1981).

119. Vasil'ev, V. P. and Zaitseva, G. A., Russ. J. Inorg. Chem. **13**, 42 (1965).
120. Pershina, V., Radiochimica Acta **80**, 75 (1998).
121. Dullmann, C. E., Folden, C. M., Gregorich, K. E., Hoffman, D. C., Leitner, D., Pang, G. K., Sudowe, R., Zielinski, P. M., and Nitsche, H., Nuc. Instr. Meth. in Phys. Rec. A **551**, 528 (2005).
122. Eichler, R., Bruchle, W., Buda, R., et al., Radiochim. Acta 94, 181 (2006).
123. Yakushev, A., Private Communication (2006).
124. Guillaumont. R. and Miranda. C., edited by Marcus, Y., Marcel Dekker, New York 1971), Vol. 1, p. 105.
125. Marcus, Y. and Kertes, A. S., in *Ions Exchange and Solvent Extraction of Metal Complexes* (Wiley-Interscience, London, 1969), p. 960.
126. Baes, J. C. F. and Mesmer, R. E., *The hydrolysis of Cations* (John Wiley, New York, 1976).